



**HAL**  
open science

## Macro- and micronutrient release from ash and litter in permafrost-affected forest

Daria Kuzmina, Sergey V Loiko, Artem G Lim, Georgy I Istigechev, Sergey P Kulizhsky, Frederic Julien, Jean-Luc Rols, Oleg S Pokrovsky

### ► To cite this version:

Daria Kuzmina, Sergey V Loiko, Artem G Lim, Georgy I Istigechev, Sergey P Kulizhsky, et al.. Macro- and micronutrient release from ash and litter in permafrost-affected forest. *Geoderma*, 2024, 447, pp.116925. 10.1016/j.geoderma.2024.116925 . hal-04908134

HAL Id: hal-04908134

<https://ut3-toulouseinp.hal.science/hal-04908134v1>

Submitted on 23 Jan 2025

**HAL** is a multi-disciplinary open access archive for the deposit and dissemination of scientific research documents, whether they are published or not. The documents may come from teaching and research institutions in France or abroad, or from public or private research centers.

L'archive ouverte pluridisciplinaire **HAL**, est destinée au dépôt et à la diffusion de documents scientifiques de niveau recherche, publiés ou non, émanant des établissements d'enseignement et de recherche français ou étrangers, des laboratoires publics ou privés.



Distributed under a Creative Commons Attribution 4.0 International License



## Macro- and micronutrient release from ash and litter in permafrost-affected forest

Daria Kuzmina<sup>a</sup>, Sergey V. Loiko<sup>a</sup>, Artem G. Lim<sup>a</sup>, Georgy I. Istigechev<sup>a</sup>, Sergey P. Kulizhsky<sup>a</sup>, Frederic Julien<sup>b</sup>, Jean-Luc Rols<sup>b</sup>, Oleg S. Pokrovsky<sup>c,\*</sup>

<sup>a</sup> BIO-GEO-CLIM Laboratory, Tomsk State University, 36 av. Lenina, Tomsk 634004, Russia

<sup>b</sup> Centre de Recherche Biodiversité et Environnement, Université de Toulouse, CNRS, Toulouse INP, Université Toulouse 3 – Paul Sabatier (UPS), Toulouse, France

<sup>c</sup> GET UMR 5563 CNRS University of Toulouse (France), 14 Avenue Edouard Belin, 31400 Toulouse, France

### ARTICLE INFO

Handling Editor: A. Agnelli

**Keywords:**  
Permafrost  
Peatland  
Wildfire  
Carbon  
Nutrient  
Metal

### ABSTRACT

The impact of wildfire on terrestrial and aquatic ecosystems in permafrost-affected regions is a major and still poorly understood consequence of climate warming in high latitudes. Towards better characterization of processes controlling post-fire nutrient migration and to establish the relationship between forest litter and aquatic systems during a fire event, we studied organic and inorganic solute leaching from ash that was produced via burning organic litter (topsoil) collected in permafrost-affected forest in western Siberia. Litter samples were burned at 300, 450 and 600 °C and dissolved organic carbon (DOC), major elements (Ca, Mg, Cl, SO<sub>4</sub>, Na, N, P, K, Si), carboxylic organic acids, and ~ 40 trace elements were analyzed in leachates (<0.45 μm and < 3 kDa) produced from ash reacting with water. The ashing temperature was one of the major factor controlling solute release to the aqueous solution, notably via its impact on leachate acidity and DOC concentration. The concentrations of DOC, organic (carboxylic acids) and inorganic nutrients, cationic metal micronutrients, and low-mobility geochemical tracers decreased with an increasing of ashing temperature. In contrast, labile anionic-group elements and alkaline metals were preferentially released at high ashing temperature. We also performed batch leaching of fresh (unburned) litter samples under identical experimental conditions. Results demonstrated that ash obtained from burning soil litter samples is less reactive than fresh litter. In particular, the majority of inorganic nutrients and carboxylic acids exhibited a factor of 3 to 10 higher mass-normalized yield to aqueous solution from fresh litter compared to that from ash. It follows that the fire severity is one of the main factors controlling organic and inorganic nutrient release from ash to soil and surface water. Results of the present study may help to foresee possible consequences of wildfire regime changes in permafrost regions on biogeochemical cycles of organic and inorganic macro- and micronutrients between the forest/tundra biomes and adjacent aquatic ecosystems.

### 1. Introduction

Despite a general agreement that fires are the primary destabilizing factor in high latitude biomes (Kasischke et al., 2005; Kasischke and Turetsky, 2006; Hu et al., 2015; Kharuk et al., 2021; Nelson et al., 2021; Talucci et al., 2022; Potter et al., 2023), the magnitude of wildfire impact on element cycling in terrestrial and adjacent aquatic ecosystems remains poorly understood. In these regions, the climate warming is capable of increasing the wildfire area, frequency and severity therefore modifying element cycling in the soil profile and downstream river export. Currently, wildfires are rapidly expanding into boreal forests

with emerging warmer and drier fire seasons, accounting for 10 % of global fire carbon dioxide emission (i.e., Zheng et al., 2023). Wildfires in permafrost regions are especially important given that these territories store sizable proportions of carbon (C) in the form of aboveground biomass, surface litter, and soil organic and mineral layers (Botch et al., 1995; Czimczik et al., 2003; Beilman et al., 2009; Ackley et al., 2021; Gao et al., 2023). Thus, while it is known that wildfires are among the most important driving forces for permafrost carbon release into the atmosphere (Chen et al., 2021; Heim et al., 2022; Miner et al., 2022), the fate of other constituents in burned organic matter (macro- and micronutrients) in permafrost impacted terrestrial and aquatic ecosystems is

\* Corresponding author.

E-mail address: [oleg.pokrovsky@get.omp.eu](mailto:oleg.pokrovsky@get.omp.eu) (O.S. Pokrovsky).

<https://doi.org/10.1016/j.geoderma.2024.116925>

Received 25 October 2023; Received in revised form 6 May 2024; Accepted 17 May 2024

Available online 21 May 2024

0016-7061/© 2024 The Author(s). Published by Elsevier B.V. This is an open access article under the CC BY license (<http://creativecommons.org/licenses/by/4.0/>).

rather elusive.

The main unanswered question is to what extent do climate warming induced increases in wildfire area, fire frequency and fire severity in high latitudes (Flannigan et al., 2000; Kasischke et al., 2010, Ludwig et al., 2018; Novenko et al., 2022) modify elemental (C, macro and micronutrients, major and trace elements including pollutants) cycling in the soil profile and downstream river export. Although these elements are vulnerable to post-fire leaching into and through the soil and drainage to downstream waterbodies (Christensen, 1973, Grier, 1975, Kauffman et al., 1993; Burke et al., 2005; Petrone et al., 2007; Wu et al., 2022), there remain significant questions as to what determines magnitude and temporal dynamics of post-fire elemental release at the watershed scale (Ackley et al., 2021; Granath et al., 2021). On a worldwide scale, meta-analysis demonstrated strong heterogeneity in responses of water quality to wildfires in forested catchments (e.g., Rust et al., 2018; McCullough et al., 2019; Basso et al., 2020; Crandall et al., 2021; Mishra et al., 2021; Hampton et al., 2022). Several studies have addressed the impact of fire on dissolved organic carbon (DOC), major elements and nitrate in stream water across fire chronosequences in larch forests of Central Siberia (Kawahigashi et al., 2011, Parham et al., 2013, Diemer et al., 2015, Knorre et al., 2019; Rodriguez-Cardona et al., 2020) and boreal forest of Northern Europe (Granath et al., 2021) and Alaska (Betts and Jones, 2009). These studies demonstrated the largest impact of forest fire on stream chemistry during the first years after the fire event, with a gradual decrease over the first decade. However, studies of element dynamics in fire-impacted, permafrost-bearing ecosystems remain very limited; there exist only occasional investigations on Canadian (Burd et al., 2018; Gibson et al., 2018; Ackley et al., 2021) and European (Liu et al., 2023) peatlands.

Ash deposited on surface soils after a fire is light and loose and highly mobile by wind and water. It is particularly enriched in essential nutrients like nitrogen, sulfur, phosphorus and potassium (Harden et al., 2004; Neff et al., 2005; Koyama et al., 2010) and also some trace elements (e.g., Hredja et al., 2022). Most elements contained in plant ash are present in a water-soluble state (Pereira et al., 2012, 2017). As a result, these elements are highly mobile over the first few days to weeks after a wildfire has occurred (Christensen, 1973; Grier, 1975; Kauffman et al., 1993). Overall, through consuming a sizable amount of ecosystem organic carbon (OC) stock, wildfires accelerate the recycling of major- and micro-nutrients such as K, S, N, P, Si and trace metals (Whelan, 1995; Moilanen et al., 2002; Spencer et al., 2003). Although there were several studies on ash from moss, lichen and peat reactivity in aqueous solutions (Manasypov et al., 2017; Kuzmina et al., 2022), these works were conducted on individual species rather than on bulk soil litter that is typically subjected to ground fire. Furthermore, former studies lack comparison with initial organic biomass which is necessary to assess the relative role of ash versus non-burned vegetation in element cycling between soil and aquatic ecosystems of permafrost regions. Indeed, considering consequences of wildfires on element delivery from land to rivers, there are two counteracting factors. On one hand, ash is highly reactive and susceptible to quick contact with incoming surface flow thereby releasing its constituents into the aqueous solution. On the other hand, wildfire consumes a sizable amount of vegetation litter which is, potentially, a sizable source of macro- and micronutrients for the hydrological network. As such, a comparative study of nutrient release from fresh litter and ash is needed to quantitatively assess possible impact of wildfire on the element delivery to soil porewaters in permafrost peatlands.

As a first step towards this assessment, we chose three contrasting microtopography positions of the forested site in the discontinuous permafrost of western Siberia and performed laboratory experiments to address the following objectives. First, to quantify the yield (mass-normalized release) of organic C, macro- and micronutrients from litter ashed at 300, 450 and 600 °C into the aqueous solution, via measuring elemental concentrations in relevant leachates. Selected temperature range reflects in-situ temperatures documented during ground fire in

tundra biomes (Agafontsev and Kasymov, 2020) and in organic-rich soils of smoldering peatlands (Benscoter et al., 2011), which is, however, lower than that of the boreal forest fire (Santin et al., 2016). The second objective was to compare elemental yield from ash to that from fresh litter, in order to quantify the capacity of both ash and litter to release nutrients into the soil porewater. Finally, we aimed to quantify the concentration of total dissolved, low molecular weight (LMW) and colloidal forms of OC, major and trace elements released into aqueous solution from ash and unburnt litter, and to identify possible governing factors (pH, organic carbon) of leaching process. Although comparative studies of ash and unburnt litter reactivity in aqueous solutions relevant to temperate forest ecosystems have been occasionally performed (e.g., Pereira et al., 2014), such comparisons have never been attempted for permafrost settings.

In the forest-tundra biome of west Siberian permafrost peatlands, the dominant soil catenas include ancient flat polygons (currently, sand dunes), their slopes, and depressions, separating adjacent dunes. All these microtopographic positions are covered by recent pine forest with dwarf shrubs, lichens and mosses in the understory. We therefore hypothesized, first, that microtopography position and the dominant plant species in the litter control the release of solutes from ash [as is known from microcosm and macrocosm experiments with individual plant species (Manasypov et al., 2017; Shirokova et al., 2021; Kuzmina et al., 2022)]. We then hypothesized that ashing temperature strongly controls the yield of organic and inorganic nutrients into the aqueous solution [as demonstrated for a limited number of nutrients such as S and P (White et al., 1973; Gray and Dighton, 2006)]. Our third hypothesis was that solution pH and DOC concentration are the main indicators and potential factors affecting cation and anion release to the aqueous solution from reacting ash or litter [as is known from numerous natural observations in undisturbed settings of western Siberia (Manasypov et al., 2017; Kuzmina et al., 2023)]. A novelty of the present study consist of characterizing not only major elements and macro-nutrients, but assessing a large suite of micro-nutrients, toxicants, and geochemical tracers, as well as organic acids capable of affecting biotic functioning of surface waters.

## 2. Methods

### 2.1. Environmental context of sampling sites

Despite the fact that wildfire effects are very heterogenous, the ground fires in the forest-tundra biome typically consume the upper 10 cm ( $\pm 5$  cm) of the organic (litter) layer (e.g., Liljedahl et al., 2007; Maximova and Abakumov, 2017; Abakumov et al., 2020; Mergelov et al., 2020; Loiko et al., 2022). In August 2021, which is the period of maximal wildfire in western Siberia, we collected organic litter in three main microtopography position, in the vicinity of the Khanymey Research station (INTERACT Network, 63°47'N, 75°43'E) of the permafrost-affected part of the western Siberian Lowland (WSL). The catena is located within a former polygonal tundra, which was subjected to intense ice wedge thaw over last 10,000 years and aeolian processes that smoothed initial micro-relief and initiated pine forest growth (Velichko et al., 2011) (Fig. 1). The typical microlandscape settings are convex forms, similar to sand dunes in Alaska (Lea and Waythomas, 1990; Mann et al., 2002). Three microtopography positions include upland (top of ancient polygon), its slope and a depression which separates two adjacent uplands. The studied territory of permafrost peatlands (1941 km<sup>2</sup>, middle reaches of the Pyakupur River) is partially covered by pine forest (229 km<sup>2</sup>). Globally, the Pyakupur watershed is comprised of flat mound palsas (28 %), fens (sedge-moss depressions, 7.2 %), river floodplains (15 %), forested areas (11.8 %), khasyreys (drained lakes, 15.8 %), and thermokarst lakes (22.2 %). Within the key site of forested region, the surface coverage contribution of upland, slope and depression is 35.2, 51.5 and 13.4 %. Generally, a combination of upland-slope-depression constitutes typical soil catenas in northern

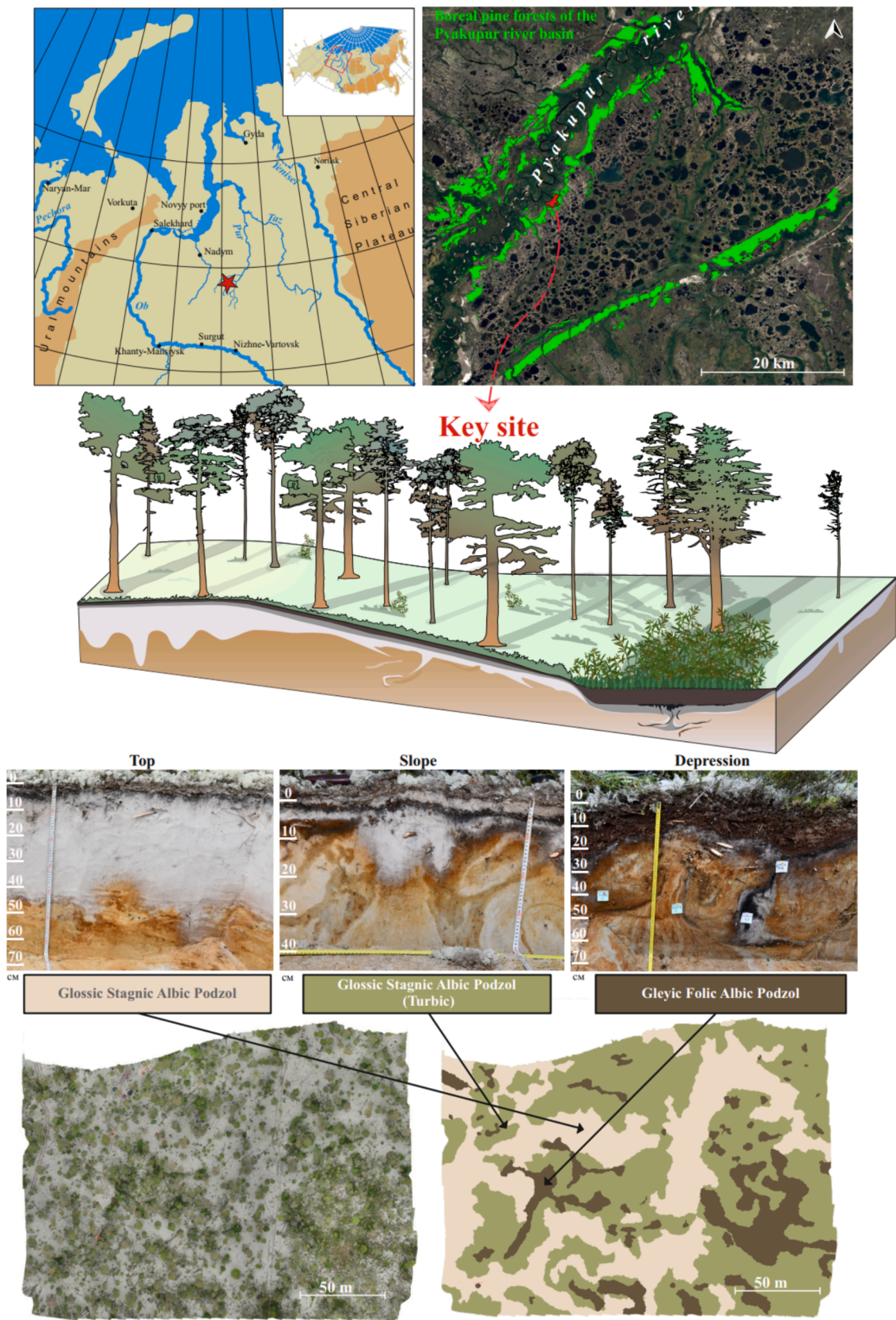


Fig. 1. Location of the study site, three main microtopography positions with relevant soil transects, relief from the orthophotomap and soil distribution on the catena.

Europe and Siberia (Goryachkin et al., 2010).

The upland and slope exhibited similar soil coverage that can be defined as Glossic Stagnic Albic Podzol (according to WRB 2014). The difference between soils in these microtopographic landforms is that the Upland Podzols are twice as thick with regards to their Albic horizon compared to slope soils. Sparse lichenized pine forests with mixtures of blueberries and lingonberries grow across the uplands. Slopes are covered by denser shrub-lichen pine forests with solitary birches and larches. Depressions are comprised of pine forests with wild rosemary, dwarf birch, and green moss. The depressions are covered by Gleyic Folic Albic Podzol with organic Folic horizons over 10 cm thick.

First of all, we made sure that sampled microtopography positions are representative for the entire region of Pyakopur peatlands, located in the discontinuous permafrost zone. For this, we examined three independent dunes, three slopes and three depressions located within several km distance between each other. Based on ground observations and pedological examination of soil profiles, we found them fairly identical in terms of soil type, litter thickness ( $\pm 3$  cm) and the proportions ( $\pm 10$

%) of dominant vegetation. Prior choosing the test plots for fresh litter sampling, large rectangular profiles of litter and soil (2 x 2 m size, 1 m deep) were created in each component of the selected microtopography position) as illustrated in Fig. S1 of the Supplement.

Three microtopography positions included 1) the upland (top of the dune, labelled 'T'), developed on Glossic Stagnic Albic Podzol that was covered by pine trees [*Pinus sylvestris*, and less often *Pinus sibirica* and *Larix sibirica*] with dwarf shrubs [*Vaccinium vitis-idaea*, *Ledum palustre*] and understored lichens [*Cladonia* sp.]; T litter was dominated by lichens (90 %), occasionally was comprised of < 10 % of lichen-pine needle combination, and rarely contained < 2 % pine bark, branch debris and intermixed pine cones; 2) the slope (labelled 'S') was covered by more dense pine trees and dwarf shrubs [with equal proportions *Vaccinium vitis-idaea*, *Vaccinium myrtillus* (blueberry) and *Empetrum* sp. (crowberry)], developed on Glossic Stagnic Albic Podzol (Turbic); S litter was dominated by pine needles intermixed with dwarf shrub leaves and roots (60 %) with lesser proportions of lichens (35–40 %); 3) the depression (labelled 'D'), located at the intersection of two paleo-cracks

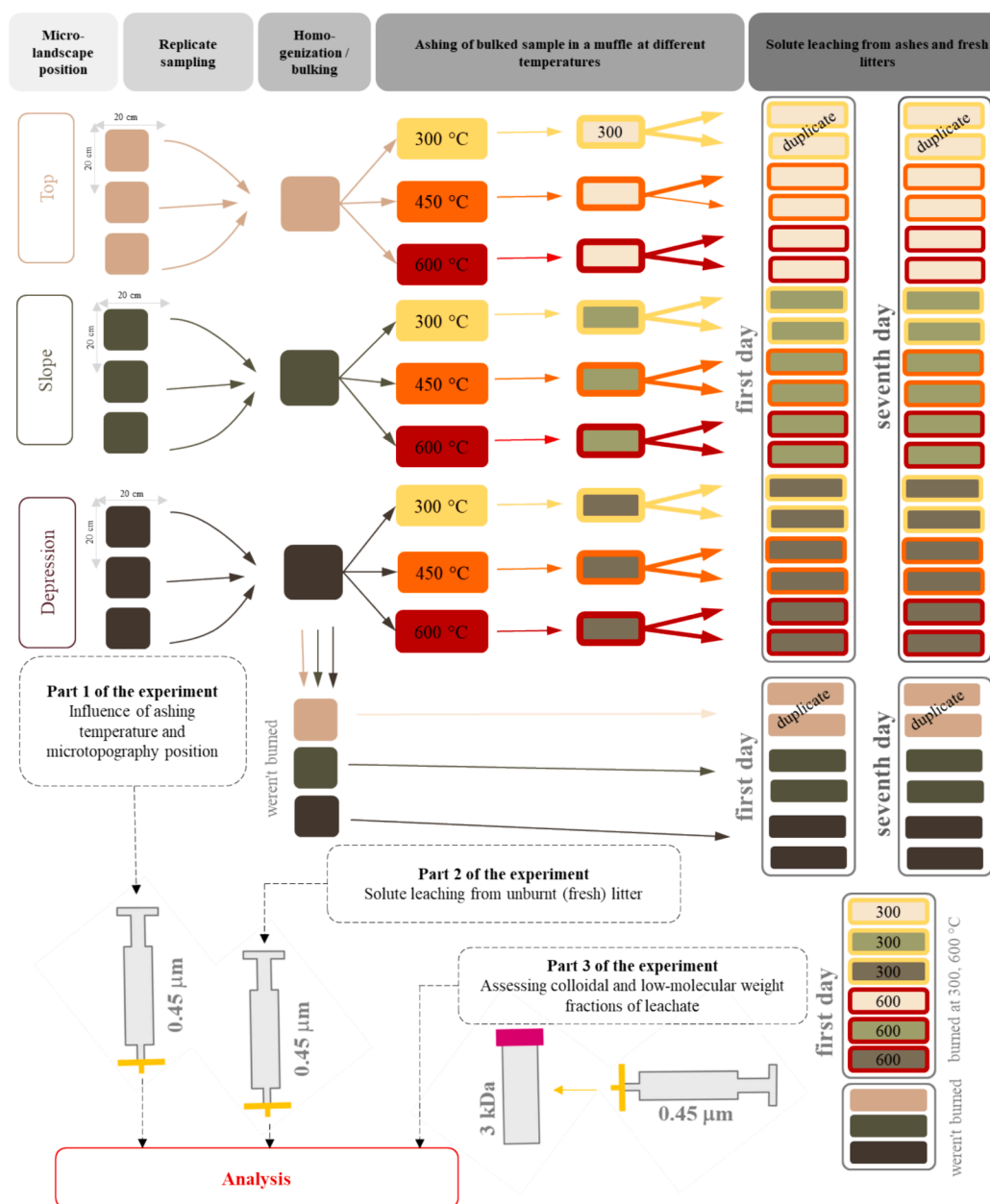


Fig. 2. Scheme of litter sampling, ashing, experimental set-up and analyses of solutes.

between polygons, developed on Gleyic Folic Albic Podzol and covered by pine trees and evergreen shrubs (*Ledum* sp.) with understored green mosses; D litter was dominated by green mosses, evergreen leaves and roots, and wood and bark debris of pine in addition to a small proportion (5–15 %) of lichens.

The scheme of initial material preparation and conducted experiments is provided in Fig. 2. Litter layer was sampled via removing upper 0–10 cm of organic horizon over the surface of a 20 x 20 cm rectangle. At each microtopography position, these rectangles were made in triplicates at a distance of  $10 \pm 5$  m from each other and collected samples were pooled together, via mechanical mixing without grinding, to create a maximally representative composite samples of litter in each microtopography position. Note that bulking of soil samples is commonly used to obtain a spatially averaged measure of soil properties (i.e., Giesler and Lundström, 1993). After sampling, litter was rinsed in Milli-Q water in order to remove admixtures of atmospheric dust, following standard procedures of organic plant material conditioning prior to chemical treatment (e.g., Delplace et al., 2020). This allowed to create a stock of homogeneous material and use it for comparative study of ash and non-burned litter leachate chemistry as described below.

## 2.2. Ash preparation

The litter was dried at 30 °C for 3 weeks using Osmofilm® bags till constant weight. The use of osmofilm allowed to preserve the intact state of the litter and prevented it from external contamination during drying. Regardless of the microtopography, the residual moisture was equal to  $7.7 \pm 0.75$  % of total weight and it was explicitly taken into account when calculating element yields. We placed 100 g of dry non-ground litter in acid and MQ-cleaned porcelain cups (5 cm diameter, 10 cm height) and exposed them, over 3 h separately at 300, 450 and 600 °C in a Vecstar® furnace, by gradually raising the temperature from ambient to the target temperature over 0.5 h, followed by a 1 h period at the target temperature, after which the sample was cooled to ambient temperature for a period of 1.5 h. The total of 3 h duration time of thermal treatment is a reasonable compromise between fast ground fire event, when the fire front propagates with a rate of several cm per second (Thomas et al., 2021; Filkov et al., 2023), and slow smoldering of upper peat horizons in non-permafrost regions (e.g., Liu et al., 2023). While the first regime is typical for slope and upland microtopography position, the second one is typical for studied depressions. By applying this treatment, we expected a difference in component volatility and residual OM content at different ignition temperatures, hence covering the natural range of possible environmental conditions during ground fire events.

Ashing of litter at 300 and 450 °C produced a material of black color presumably indicating an incomplete combustion (Bodi et al., 2014) whereas the ash produced at 600 °C was grey to white. The ash content of the litter (T, S and D sites) ranged from 10–20 % during ashing at 300 °C (i.e., 80–90 % reduction in mass with ashing at 300 °C) to 2–3 % during ashing at 600 °C, as measured in three independent litter samples, collected from each microtopography position.

## 2.3. Ash and litter incubation experiments

Measurements of ash and fresh (unburned) litter constituent release into aqueous solution were performed at a concentration of 100 g<sub>dry</sub> ash/litter per liter of water, in 50-mL sterile acid cleaned Nalgene polypropylene vials. Preliminary tests at 10, 20 and 50 g<sub>dry</sub> L<sup>-1</sup> demonstrated similar pH, DOC and specific conductivity level in leachates produced after several days of reaction. Note that the 1:10 solid:water ratio was chosen for consistency with previous studies of our group on ash of individual plants and peat (Kuzmina et al., 2022; 2023) and typical leaching test at 1:20 used in other studies of ash leaching (Hageman et al., 2007). In a previous methodological work with soil leachates in the laboratory and native soil porewaters in this region, we

demonstrated an adequacy of using both 1:10 and 1:100 solid:liquid ratios, with best approximation of soil fluids achieved at 1:10 ratio (Kuzmina et al., 2023). Finally, the litter:water and ash:water ratio of 1:10 used in the present study is consistent with typical porewater content in peat surface horizons of 10 %, as observed in the field at the Khanymey Research Station (Raudina et al., 2018), water holding capacity of bryophyte species in western Siberia (Volkova et al., 2023), and recent laboratory experiments on water leaching of smoldered peat (Liu et al., 2023). We acknowledge, however, that natural dilution during post-fire rain events in both surface and subsurface conditions can be sizably higher.

Experiments were run in duplicates, i.e., two parallel reactors for each type of ash and litter, using samples from T, D and S microtopography position. Vials were shaken for one week on a ping-pong shaker (100 rpm) at  $20 \pm 0.5$  °C in darkness. After 1 and 7 days of incubation, the contents of each vial were entirely sacrificed for chemical analyses. We used two different exposure times to account for kinetics of reaction, verify the steady-state concentration achievement, and encompass typical water residence / travel time (several days) in surface and subsurface conditions of Siberian permafrost peatlands (e.g., Raudina et al., 2017, 2018), including post-fire conditions (Parham et al., 2013). Further, the exposure of 1 and 7 days was based on previous methodological studies (Kuzmina et al., 2022) where it was demonstrated that the majority (>80–90 %) of inorganic constituents were leached from ash of permafrost peatland vegetation and peat during  $1.5 \pm 0.5$  days of exposure, while the rest of solutes were mobilized over the remaining  $7 \pm 2$  days of reaction.

Suspensions were filtered using a sterile syringe and a disposable, single-use 0.45 µm Millipore filter unit. We also tested the presence of colloidal forms of solutes and assessed the concentrations of low molecular weight (<3 kDa) fraction ( $LMW_{< 3 \text{ kDa}}$ ) using a conventional size separation procedure (e.g., Raudina et al., 2021; Lim et al., 2022). The ultrafiltration through 3 kDa pore size was performed using Amicon Ultracel® centrifugal filters made of regenerated cellulose. The disposable 50-mL polypropylene vials were first treated with 1 % HNO<sub>3</sub> and rinsed 3 times via passing between 50 and 100 mL of MilliQ water through the membrane. The DOC, organic and inorganic nutrients, and trace metal blanks were a factor of 3 to 10 lower than the minimal concentrations of these components in experimental leachates.

## 2.4. Chemical analyses

The pH and electrical conductivity were measured using Hanna portable instruments. DOC, organic and inorganic anions, and major and trace elements were measured in both 0.45-µm filtrates and 3 kDa –ultrafiltrates. Fifteen carboxylic acids which are relevant to soil porewater environments and can be used as labile organic matter by aquatic microorganisms (quinic, lactate, acetate, propionate, formate, butyrate, galacturonate, glutarate, malate, tartrate, maleate, oxalate, fumarate, phthalate and citrate) and main inorganic anions (F<sup>-</sup>, Br<sup>-</sup>, Cl<sup>-</sup>, SO<sub>4</sub><sup>2-</sup>, NO<sub>3</sub><sup>-</sup>, NO<sub>2</sub><sup>-</sup> and PO<sub>4</sub><sup>3-</sup>) were measured by high-performance ionic chromatography (Dionex Ics-5000 + ) with an uncertainty of 2 %. We used an in-house standard for organic acid analysis and two ISO standards (ISO 10304–1 and ISO 10304–2) for inorganic anion analysis. The certified reference materials Ion-915 and Ion-964 were used to verify the accuracy of analyses; the reference material measured concentrations were within 10 % of certified values. Quantification limits were equal to 0.05 mg L<sup>-1</sup> for Cl<sup>-</sup>, 0.001 mg L<sup>-1</sup> for F<sup>-</sup>, Br<sup>-</sup>, PO<sub>4</sub><sup>3-</sup>, 0.01 mg L<sup>-1</sup> for NO<sub>3</sub><sup>-</sup>, SO<sub>4</sub><sup>2-</sup> and 0.002 mg L<sup>-1</sup> for quinate, lactate, acetate, propionate, formate, butyrate, galacturonate, glutarate, malate, tartrate, maleate, oxalate, fumarate, phthalate and citrate.

DOC and dissolved inorganic carbon (DIC) were determined by a Shimadzu TOC-VSCN Analyzer with an uncertainty of 3 % and a detection limit of 0.1 mg/L. Specific UV absorbance (SUVA) was measured as absorbance at 254 nm normalized for DOC concentration in L mg<sup>-1</sup> m<sup>-1</sup>. Major cations (Ca, Mg, Na, K), Si and ~ 45 trace elements

were determined with an Agilent iCap Triple Quadrupole (TQ) ICP MS using both Ar and He modes to diminish interferences. About 3 µg/L of In and Re were added as internal standards along with 3 various external standards, which were placed each 20 experimental samples. Detection limits of trace elements (TE) were determined as 3 times the blank signal. The typical uncertainty for elemental concentration measurements was 5 % at 1–1000 µg/L and 10 % at 0.001–0.1 µg/L. The Milli-Q blanks were routinely processed to monitor for any potential contamination introduced by our sampling and handling procedures. The SLRS-6 (Riverine Water Reference Material for Trace Metals certified by the National Research Council of Canada) was analyzed every 20 samples to check for accuracy and reproducibility of analyses (Yeghicheyan et al., 2019). All certified elements exhibited good agreement between replicated measurements of SLRS-6 and the certified values (with relative difference < 10–15 %).

Total (bulk) chemical composition of fresh litter and ash was measured using an X-ray Fluorescence spectrometer (X Bruker S2), via fusing with Li borate after ashing the dry material at 1200 °C (XRfuse6, Bruker). We used a set of 7 sediment and rock standards to quantify major elements (i.e., Mg, Na, Si, Al, P, S, K, Ca, Mn, Ti, Fe) with an average uncertainty of 1 %. Concentrations of these elements were in agreement with certified values of geostandards (within ± 10 %).

### 2.5. Data treatment: Statistical tests and thermodynamic modelling

Due to low number of parameters and variables, the ANOVA conditions were not met, and the data were not distributed normally. The differences between data sets (solute concentrations in leachates and mass-normalized yields) corresponding to the role of the microtopography position, ashing temperature and incubation time were tested using Mann-Whitney *U* test, which allows to test one factor at a time. Note that the Tukey (HSD, HSD for unequal *N*) test was not suitable for our data set. Therefore, to assess the impact of both temperature and microtopographic position on chemical composition of solutes, we tested separately the effects of microtopography position (MP) for each temperature of ashing ( $T_{\text{ashing}}$ ) and each time of exposure. The tests were performed at a significance level of 95 %. Further, the Pearson correlations between major leachable constituents of ash, such as  $\text{SO}_4$ , Si, P, K, Al, Fe, Ca, DIC, DOC, pH and trace element were considered significant at  $p < 0.05$  (SigmaPlot version 11.0, Systat Software, Inc). The mass normalized yields of component by ash and fresh litter were calculated for the first 1 and 7th day of reaction.

Element speciation and solution saturation state with respect to possible solid phases in the experimental solutions were assessed using the Visual MINTEQ computer code (Gustafsson, 2014; version 3.1 for Windows following the procedure for surface waters of boreal and permafrost landscapes (Raudina et al., 2021). The input parameters of the model were the solution temperature, pH, DIC, DOC, major anions, cations, and trace metal concentrations. The model provided a degree of solution supersaturation with respect to possible solid phases (hydroxides, oxides, carbonates and phosphates of Ca, Mg, Fe(III), Al, and some trace metals).

## 3. Results

### 3.1. Chemical composition of ash

Ash content of the studied organic substrates followed the order: Upland > Slope > Depression, and systematically decreased with an increase in burn temperature. Total chemical analysis of solid ash performed by XRF demonstrated a high proportion (30–50 %) of Si, followed by Al, Fe, Ca, K, S, P, Ti, Na, Mg and Mn (Table S1). There were no significant differences in element concentration in 300 °C ash of litter from the upland and the slope (Mann-Whitney test,  $p < 0.05$ ). Ash produced at 450 and 600 °C from the S litter demonstrated two to three times higher concentrations of Na, Mg, Al, K, and Mn compared to ash of

the upland litter. The litter of the depression (D) was strongly (a factor of 2 to 10) enriched in all major constituents except Si compared to litter from the top and slope microtopography position.

### 3.2. Release of organic and inorganic constituents from ash obtained at different temperature

The microtopography position (upland, slope or depression) exhibited rather weak control on solute release from relevant ash. First, regardless of the MP, there was a drastic effect of burning temperature on ash constituent release (Table 1). There was a strong (a factor of 7) increase in aromaticity of DOM ( $\text{SUVA}_{254}$ ) and decrease (a factor of 40) in DOC concentration with ashing temperature (Fig. 3 A, B). The pH of leachates increased by about 2 units when the litter ashing temperature increased from 300 to 600 °C (Fig. 3 C). This rise in pH was most likely linked to a decrease of the proportion of residual acidic organic matter in the ash produced at higher temperatures. The impact of ashing temperature on release of organic and inorganic solutes was fairly similar among all three sampling sites (upland, slope and depression). For each MP, ashing temperature significantly ( $p < 0.05$ ) impacted most element concentration in the leachates (Table S2 of the Supplement).

Two groups of solutes were distinguished based on pattern of solute concentration dependence on the ashing temperature. The first solute group containing DOC, most carboxylates, F, phosphate and trace metals (divalent metals, trivalent and tetravalent hydrolysates, known to be strongly bound to organic matter in the form of colloids) decreased their concentration by 10 to 20 times for leachates of ash produced at 300 and 600 °C (Table 1, Fig. 4). The second solute group was represented by labile soluble major and trace elements that are present as anions or neutral molecules, some carboxylates (e.g., fumarate, galacturonate), alkaline and alkaline-earth metals, which showed either indifferent behavior or an increasing yield with an increase in ashing temperature (Table 1, Fig. 5). These elemental groups were identified by their degree of yield from ash into aqueous solution and were confirmed by pairwise (Pearson) correlations (Table 2). Considering all sampling sites together, in the leachates, labile elements (B, Na, V, Se, Mo, Rb, Cs, Sb) strongly correlated with K ( $p < 0.01$ ) as the dominant cation in the solution whereas immobile elements (Ti, Zr, Y and REEs) correlated with Fe and DOC ( $p < 0.01$ ).

Tests on the effect of incubation time on leachate concentrations demonstrated that the difference in solute concentration between 1 and 7 day of reaction was not systematically pronounced. A general increase in concentration (a factor of  $1.45 \pm 0.45$ ) was observed for ash produced at 300 °C. The effect of exposure time was much less pronounced for the 450 and 600 °C ash; the average ratio of 68 component concentrations after 7 days of exposure to that after 1 day of exposure was equal to  $1.14 \pm 0.30$  (Table S3 of the Supplement). The concentration of Fe and Si sizably (a factor of 2 to 2.5) increased from the 1st to the 7th day of reaction. Note that thermodynamic calculation of the solution saturation state with respect to possible major solid phases (hydroxides, carbonates and phosphates of Ca, Mg, Fe(III) and Al) did not demonstrate oversaturation ( $\text{S.I.} < -1.0$ ). The main reasons for that are relatively high acidity ( $\text{pH} = 4.0\text{--}6.0$ ) and the presence of DOM from ash residue, which acted as strong complexant, hence stabilizing dissolved  $\text{Fe}^{3+}$  and  $\text{Al}^{3+}$  in oxygenated aqueous solutions and preventing precipitation of insoluble Ca phosphates and carbonates. Testing the presence of colloidal forms of solutes (3 kDa – 0.45 µm) in ash leachates demonstrated a generally weak (<20–30 %) proportion of colloids in the total dissolved (<0.45 µm) fraction of major and trace elements, regardless of the microlandscape and ashing temperature (Table S4 of the Supplement).

### 3.3. Element leaching from fresh (unburned) litter and solute yield comparison

Similar to ash, the release of fresh litter constituents to the aqueous solution occurred in the course of first hours to days. Concentrations of

**Table 1**

Element yield (mean  $\pm$  s.d.) from ashes prepared at different temperatures and fresh litter to aqueous solution (averaged across sites) over 7 days of reaction.

| Parameter                       | 300°C                    | 450°C      | 600°C       | Litter                           |
|---------------------------------|--------------------------|------------|-------------|----------------------------------|
|                                 | $\mu\text{g g}^{-1}$ ash |            |             | $\mu\text{g g}^{-1}$ dry biomass |
| DOC                             | 2170                     | 255        | 53.1        | 9530                             |
| SUVA <sub>254</sub>             | 0.55                     | 1.09       | 3.70        | 0.66                             |
| DIC                             | 32                       | 28.9       | 97.2        | 33.8                             |
| F <sup>-</sup>                  | 1.67                     | 0.117      | 0.194       | 21.0                             |
| Cl <sup>-</sup>                 | 16.0                     | 10.0       | 14.2        | 39.6                             |
| Br <sup>-</sup>                 | 0.843                    | 0.903      | 1.14        | <d.l.                            |
| N-NO <sub>3</sub> <sup>-</sup>  | 0.767                    | 0.773      | 0.674       | <d.l.                            |
| N-NO <sub>2</sub> <sup>-</sup>  | 0.08                     | <d.l.      | 0.116       | 0.945                            |
| SO <sub>4</sub> <sup>2-</sup>   | 123                      | 149        | 176         | 43                               |
| P-PO <sub>4</sub> <sup>3-</sup> | 192                      | 129        | 33.2        | 258                              |
| Quinate                         | 1.83                     | <d.l.      | <d.l.       | 49                               |
| Lactate                         | 2.36                     | 0.646      | 0.321       | 34.5                             |
| Acetate                         | 104                      | 71         | 0.596       | 49                               |
| Glycolate                       | 9.5                      | 2.10       | <d.l.       | 1.61                             |
| Propionate                      | 77                       | 60         | 0.17        | 44                               |
| Formate                         | 1.16                     | <d.l.      | <d.l.       | 3.19                             |
| Butyrate                        | 0.991                    | 0.271      | 0.140       | 1.78                             |
| Pyruvate                        | 0.414                    | 0.226      | 0.212       | 0.95                             |
| Galacturonate                   | 0.493                    | 0.311      | 0.306       | 82                               |
| Valerate                        | 0.457                    | 0.195      | 0.141       | 0.68                             |
| Glutarate                       | 15.3                     | 0.594      | 0.028       | 6.4                              |
| Malate                          | 20.0                     | 1.43       | 0.022       | 47.7                             |
| Tartrate                        | 1.00                     | 0.529      | 0.301       | 9.56                             |
| Maleate                         | 10.9                     | 5.90       | 0.505       | 2.06                             |
| Alpha-keto-glutarate            | 2.42                     | <d.l.      | <d.l.       | 7.82                             |
| Oxalate                         | 19.0                     | 2.84       | 0.293       | 81.2                             |
| Fumarate                        | 0.516                    | 0.565      | 0.592       | 0.77                             |
| Citrate                         | 10.3                     | <d.l.      | <d.l.       | 209                              |
| Li                              | 0.0654                   | 0.113      | 0.125       | 0.0188                           |
| Be                              | 0.00025                  | 0.00030    | 0.000098    | 0.00066                          |
| B                               | 0.499                    | 0.823      | 1.39        | 0.223                            |
| Na                              | 14.8                     | 19.04      | 17.9        | 12.9                             |
| Mg                              | 39.4                     | 44.5       | 30.1        | 25.9                             |
| Al                              | 19                       | 2.43       | 0.0769      | 57.02                            |
| Si                              | 28                       | 64.7       | 84.7        | 18.1                             |
| P                               | 140                      | 96         | 23.21       | 146                              |
| K                               | 254                      | 279        | 309.15      | 338                              |
| Ca                              | 130                      | 111        | 89.0        | 70.7                             |
| Sc                              | 0.00058                  | < d.l.     | 0.00070     | 0.00095                          |
| Ti                              | 0.0122                   | 0.00419    | 0.00196     | 0.0535                           |
| V                               | 0.00982                  | 0.00277    | 0.0500      | 0.0764                           |
| Cr                              | 0.00915                  | 0.00188    | 0.000695    | 0.0573                           |
| Mn                              | 7.12                     | 3.24       | 1.01        | 5.42                             |
| Fe                              | 11.6                     | 1.42       | 0.0463      | 7.67                             |
| Co                              | 0.0122                   | 0.00355    | 0.000683    | 0.01101                          |
| Ni                              | 0.628                    | 0.00883    | 0.00598     | 0.0615                           |
| Cu                              | 0.00414                  | 0.000556   | 0.000532    | 0.0458                           |
| Zn                              | 1.19                     | 0.382      | 0.0461      | 1.27                             |
| Ga                              | 0.0016                   | 0.00022    | 0.00019     | 0.0092                           |
| Ge                              | 0.00344                  | 0.0120     | 0.0148      | 0.000483                         |
| As                              | 0.289                    | 0.285      | 0.141       | 0.0476                           |
| Se                              | 0.00584                  | 0.0185     | 0.0333      | 0.00191                          |
| Rb                              | 0.936                    | 1.09       | 1.36        | 1.34                             |
| Sr                              | 0.897                    | 0.959      | 0.808       | 0.448                            |
| Y                               | 0.00087                  | 0.00013    | 0.000044    | 0.0016                           |
| Zr                              | 0.0024                   | 0.000102   | 0.000089    | 0.0046                           |
| Nb                              | 0.00025                  | 0.0000025  | 0.0000050   | 0.0012                           |
| Mo                              | 0.000652                 | 0.00464    | 0.0700      | 0.00151                          |
| Cd                              | 0.00487                  | 0.00121    | 0.000239    | 0.00823                          |
| Sn                              | 0.00067                  | 0.00027    | 0.00033     | 0.0040                           |
| Sb                              | 0.00625                  | 0.0395     | 0.0996      | 0.002003                         |
| Cs                              | 0.00863                  | 0.0108     | 0.0148      | 0.0189                           |
| Ba                              | 1.0                      | 0.640      | 0.306       | 0.703                            |
| La                              | 0.0138                   | 0.0120     | 0.0113      | 0.00696                          |
| Ce                              | 0.00105                  | 0.000184   | 0.0000437   | 0.00249                          |
| Pr                              | 0.000139                 | 0.0000256  | 0.00000506  | 0.000323                         |
| Nd                              | 0.000594                 | 0.000122   | 0.0000271   | 0.00129                          |
| Sm                              | 0.000163                 | 0.000139   | 0.0000621   | 0.000325                         |
| Gd                              | 0.000114                 | 0.0000221  | 0.00000457  | 0.000284                         |
| Tb                              | 0.0000155                | 0.00000306 | 0.000000812 | 0.0000429                        |

**Table 1 (continued)**

| Parameter | 300°C                    | 450°C       | 600°C       | Litter                           |
|-----------|--------------------------|-------------|-------------|----------------------------------|
|           | $\mu\text{g g}^{-1}$ ash |             |             | $\mu\text{g g}^{-1}$ dry biomass |
| Dy        | 0.0000930                | 0.0000162   | 0.00000312  | 0.000267                         |
| Ho        | 0.0000207                | 0.00000384  | 0.000000771 | 0.0000586                        |
| Er        | 0.0000645                | 0.0000115   | 0.00000212  | 0.000183                         |
| Tm        | 0.0000103                | 0.00000178  | 0.000000406 | 0.0000303                        |
| Yb        | 0.0000715                | 0.0000125   | 0.00000182  | 0.000219                         |
| Lu        | 0.000011                 | 0.0000021   | 0.00000042  | 0.000036                         |
| Hf        | 0.000095                 | 0.00000059  | 0.0000017   | 0.00031                          |
| W         | 0.00121                  | 0.000662    | 0.0116      | 0.00556                          |
| Tl        | 0.00111                  | 0.000601    | 0.000247    | 0.00519                          |
| Pb        | 0.0103                   | 0.00423     | 0.00248     | 0.1007                           |
| Bi        | 0.000123                 | 0.0000244   | 0.000115    | 0.000326                         |
| Th        | 0.0000941                | 0.000000188 | 0.00000213  | 0.00287                          |
| U         | 0.0000647                | 0.0000137   | 0.00000545  | 0.000244                         |

most components were similar for 1 and 7 days of exposure, and the increase over 6 days was less than a factor of 1.3 (Table S3). As such, due to relatively high litter:water ratio (1:10), we could neglect the kinetic aspect for further characterization of solute pattern in litter leachates and considered 7-day leachates as representative for steady-state conditions.

The leachates of litter from the depression yielded the lowest pH (3) and SUVA<sub>254</sub> (0.6..0.7), highest DOC, PO<sub>4</sub>, acetate, glucolate, pyruvate, galacturonate and glutarate concentrations, but also the highest Na, Mn, Fe, Cu, Zn, Rb, Sr, trivalent and tetravalent hydrolysates. The Mann-Whitney test for the difference in element yield (concentration in water normalized per g of initial litter) among the 3 microlandscapes demonstrated the largest contrast (maximal number of solutes were significantly ( $p < 0.05$ ) different) between the upland and depression or the slope and depression; however, the lowest contrast (minimal number of solutes) were significantly ( $p < 0.05$ ) different between the upland and slope (Table S2 B).

Relevant to DOM control on element release from litter, a sizable (20 – 80 %) fraction of total dissolved (<0.45  $\mu\text{m}$ ) OC, major and trace elements were present in the colloidal (3 kDa – 0.45  $\mu\text{m}$ ) form (Table S4 of the Supplement). We tentatively distinguished two main groups of elements, depending on their affinity to the colloidal versus LMW < 3 kDa fraction. Major and trace solutes present in the form of anions, neutral molecules (B, Si, P, As, Se, Mo and Sb), and alkaline metals exhibited a low proportion of colloids, ranging from 0 to 20 %. DOC, divalent transition metals and trivalent and tetravalent hydrolysates were strongly influenced by organic colloids.

In order to compare the capacity of ash and unburned litter to release organic and inorganic solutes to aqueous solution, we calculated the mass normalized 7-days yield of all measured components (Table 1; Table S5 of the Supplement). The ratio of mean yields for main organic and inorganic constituents (across all three microlandscapes) for 300 °C and 600 °C ash and unburned litter is illustrated in histograms in Fig. 6A and 6B. It can be seen that, even for many inorganic nutrients, yields of elements from unburned litter are comparable to, or even higher (by a factor of 3 to 10) than yields from ash. In contrast, labile elements present in the form of oxyanions and neutral molecules (e.g., SO<sub>4</sub>, DIC, Sb, Mo, Ge, Si, Se, Li, B, As and W) and labile cations such as Na, Sr, Ba and Mn demonstrated a factor of 2 to 5 higher yield from ash when compared to litter. The majority of inorganic nutrients and carboxylic acids demonstrated much higher yield from plant litter compared to that from ash (Fig. 6C and 6D). Overall, these comparisons clearly demonstrate the lower capacity of litter ash to enrich the aqueous solution such as soil pore and surface waters in most nutrients compared to fresh (unburned) litter.



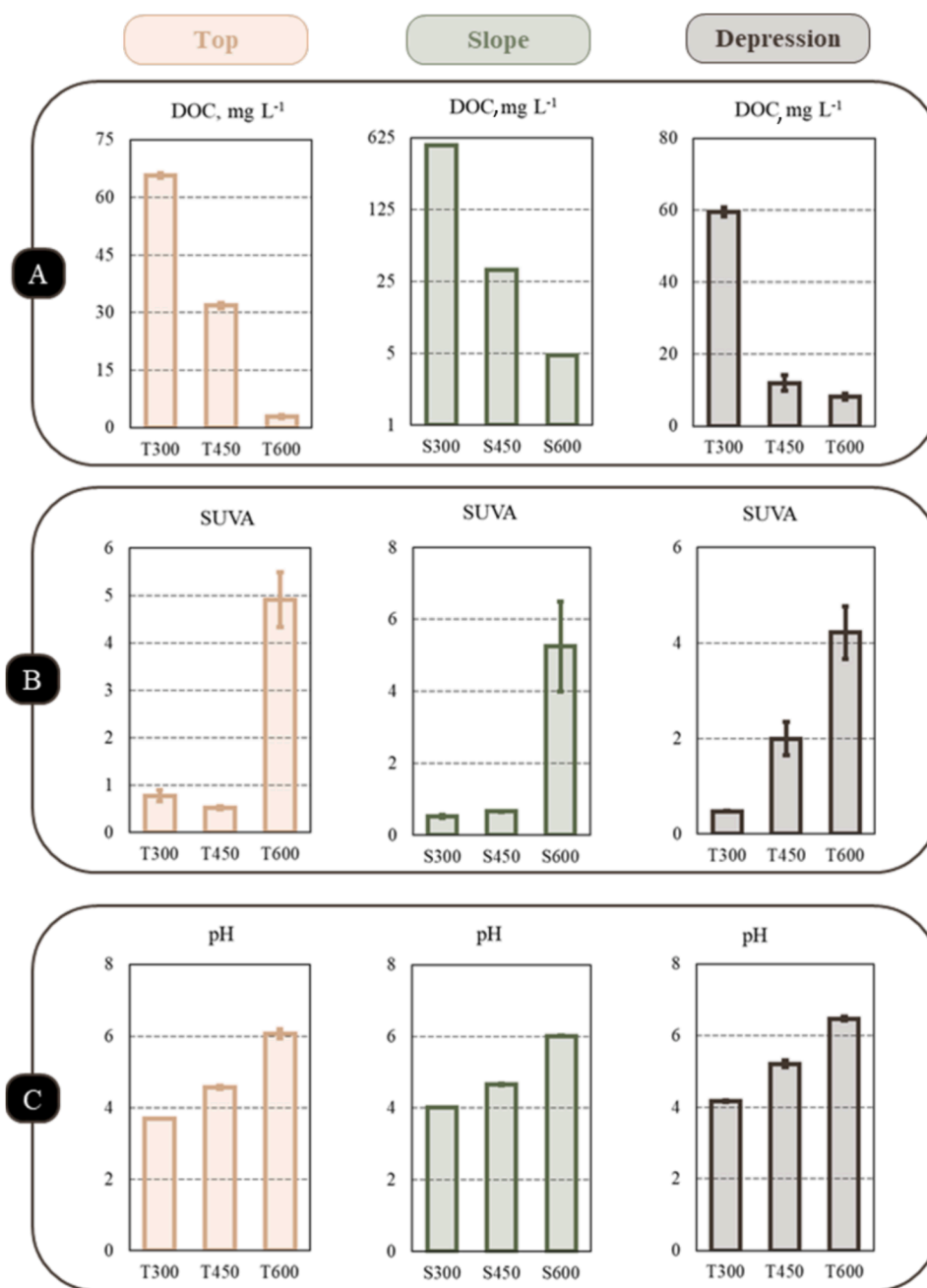


Fig. 3. DOC concentration (A), SUVA<sub>254</sub> (B) and pH (C) of leachates from ash produced at different burn temperatures in the 3 microtopography positions. Uncertainties are 2 s.d. on triplicate experiments. The units of the Y axis are mg L<sup>-1</sup> (A) and L mg C<sup>-1</sup> m<sup>-1</sup> (B).

## 4. Discussion

### 4.1. Element leachability from ashes

Fast release of ash constituents to the aqueous solution in both laboratory and natural settings is fairly well known (Bodi et al., 2014; Wu et al., 2022). Previous field mesocosm experiments in thermokarst lakes with various organic and inorganic substrates demonstrated that ash is extremely reactive in natural waters with > 90 % of its elemental stock is released over the first 10 h (Manasyov et al., 2017). Furthermore, recent high-resolution laboratory experiments showed the majority (>80 %) of labile elements mobilized from peat, moss and lichen ash over the first 10 min (Kuzmina et al., 2022). The present work corroborates these results via demonstrating fast aqueous reactivity of ashes from all three microtopography positions.

Ash formed on the surface of the soil after a fire is known to be strongly enriched in essential nutrients like N, S, P and K (Koyama et al., 2010; Harden et al., 2004; Neff et al. 2004; Pereira et al., 2012). However, the release of these macronutrients, including organic ligands (carboxylates), as well as micronutrients and toxicants depends on *i*) concentration and speciation (forms) of leachable solutes in the ash, *ii*) the pH of the aqueous solutions, which controls the solubility of solid phases and adsorption/desorption of solutes, and *iii*) the concentration of dissolved organic matter (DOM) in leachates that can mobilize major and trace cations into the aqueous solution in the form of organic colloids or complexes. First, we noted that the D litter ash was strongly enriched in Mg, P, SO<sub>4</sub>, K and Ca relative to ash of litter from the upland and slope. These highly soluble labile elements were also preferentially leached in D litter ash. Aluminium, Ti, Mn and Fe are likely to present in the form of insoluble (refractory) oxides, and they were strongly

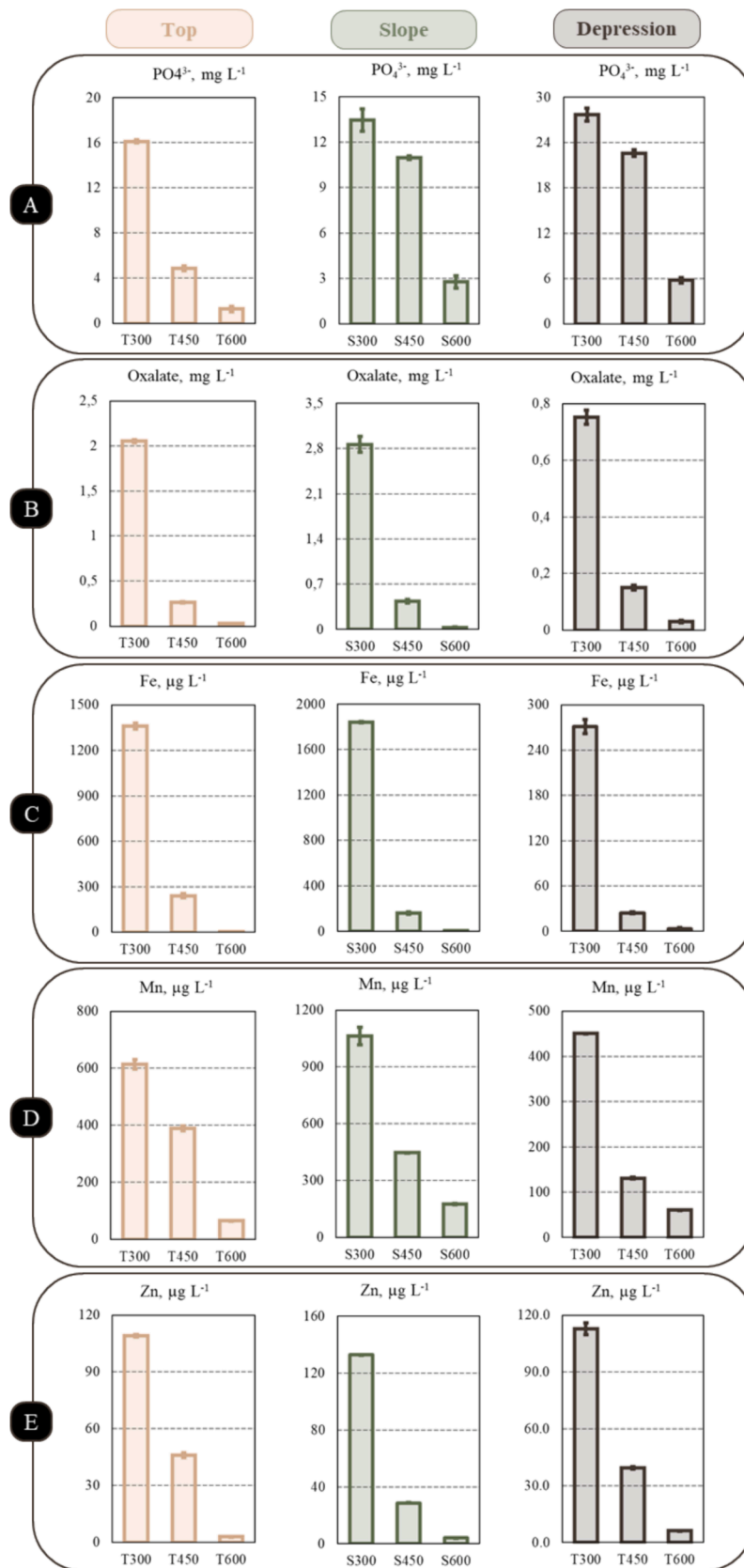


Fig. 4. Phosphate (A), oxalate (B), Fe (C), Mn (D) and Zn (E) concentration in leachates of ash produced at different burn temperatures in the 3 microtopography positions. The units of the Y axis are mg L<sup>-1</sup> (A, B) and µg/L (C, D, E).

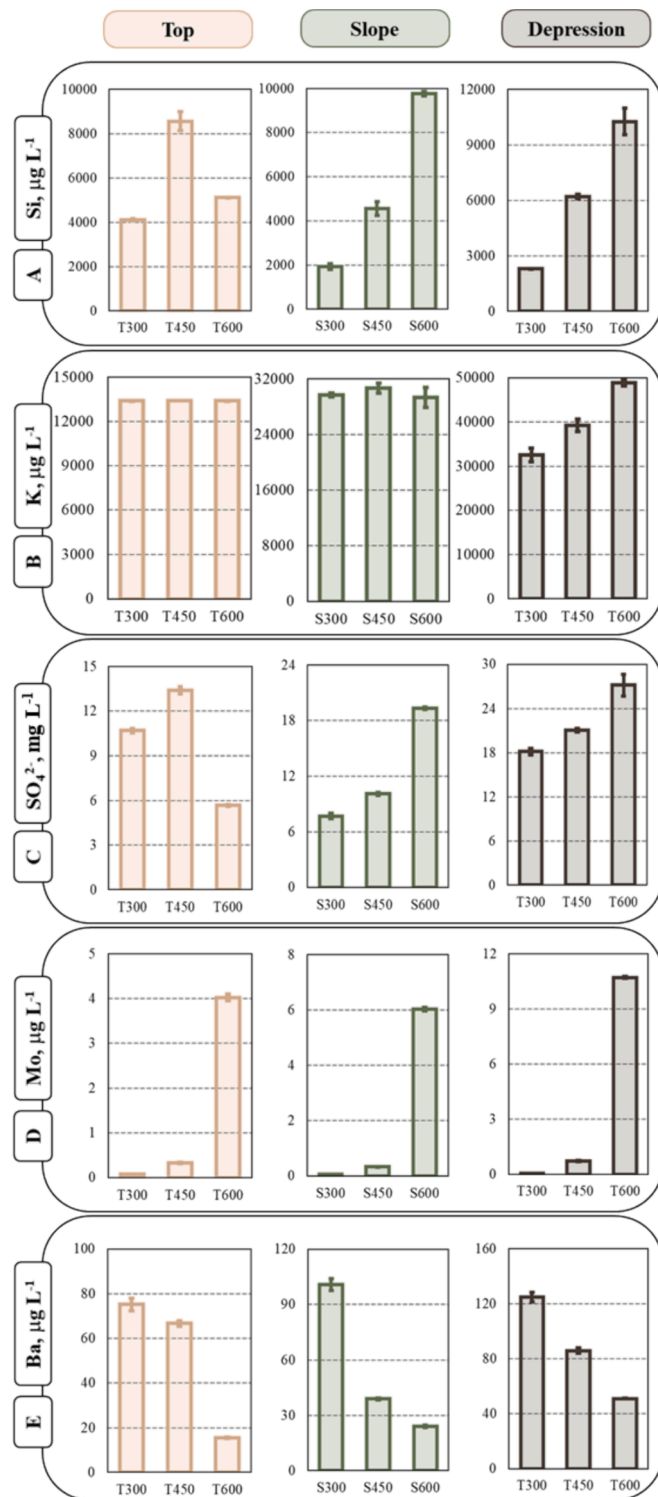


Fig. 5. Silica (A), K (B),  $\text{SO}_4$  (C), Mo (D) and Ba (E) concentrations in leachates of ash produced at different burn temperatures in three microtopography positions. The units of the Y axis are  $\mu\text{g L}^{-1}$  (A, B, D, E) and  $\text{mg L}^{-1}$  (C).

enriched in ash litter from the depression. These elements did not demonstrate any sizable variation in leachate concentrations among three studied ashes. Therefore, the release of low mobility cationic elements from the solid phase is chiefly governed by the acidity of aqueous solution and the DOM concentration in the leachates. For example, a 10-fold decrease in DOC concentration and a two-unit increase in pH between leachates of ash produced at 300 °C and that produced at 600 °C

Table 2

Pearson correlations coefficients of labile and low mobile elements with K, Fe and DOC (all ashes from three habitats treated together).

| K  | Fe    | DOC |       |    |       |
|----|-------|-----|-------|----|-------|
| La | 0.943 | Tb  | 0.935 | U  | 0.842 |
| Rb | 0.893 | Er  | 0.934 | Zr | 0.778 |
| Cs | 0.874 | Ho  | 0.934 | Fe | 0.753 |
| Se | 0.725 | Dy  | 0.933 | Ti | 0.744 |
| Sb | 0.670 | Tm  | 0.924 | Yb | 0.665 |
| Mo | 0.526 | Zr  | 0.923 | Ho | 0.664 |
| B  | 0.523 | Yb  | 0.923 | Er | 0.660 |
| V  | 0.200 | Lu  | 0.918 | Lu | 0.656 |
| Na | 0.192 | Gd  | 0.916 | Tm | 0.651 |
|    |       | Ce  | 0.903 | Dy | 0.649 |
|    |       | Pr  | 0.897 | Tb | 0.645 |
|    |       | U   | 0.887 | Gd | 0.612 |
|    |       | Nd  | 0.886 | Pr | 0.567 |
|    |       | Ti  | 0.801 | Nd | 0.563 |
|    |       | DOC | 0.753 | Ce | 0.560 |
|    |       | Y   | 0.729 | Eu | 0.469 |
|    |       | Eu  | 0.605 | Sm | 0.439 |
|    |       | Sm  | 0.444 |    |       |

For all values  $p < 0.01$

was accompanied by a concomitant decrease in concentration of elements that are likely linked to organic ligands (divalent metals, trivalent and tetravalent hydrolysates). These elements can also be adsorbed at the surfaces of insoluble solid phases dominating ash material (oxides, carbonates, black carbon) at pH 6 (ashing at 300 °C). At pH 4, corresponding to leachate of ashing at 600 °C, these elements are desorbed from ash surfaces into the solution.

In contrast, oxyanions, which are most strongly adsorbed to solid surfaces in acidic solutions, are desorbed with pH. As a result, anion concentration increases in the fluid reacted with ash of progressively increasing preparation temperature. An increase in pH and a decrease in cation concentration of leachates for high temperature ash have been reported in other studies like those on Mediterranean vegetation (Ubeda et al., 2009). In forested permafrost soils, burning at 150–200 °C resulted in decreased soil pH and increases in water-soluble organic carbon concentration when compared to ashing at 300–500 °C (Masyagina et al., 2016). A more recent study demonstrated that the peat ash may increase the soil pH in the northern temperate zone (Marcotte et al., 2022). It is important to note that the two group of elements identified above correlated either with K (labile oxyanions and alkaline metals) or organo-ferric colloids (low mobile cationic metals; rare earth elements) as shown in Table 2. Such correlations can be used for approximating relative leachability of various inorganic solutes from ash and litter in soil environments.

In ash leachates, water-extractable sulfate did not exhibit consistent behavior between 300 and 600 °C as it increased (S and D litter) and decreased (T litter). Therefore, the volatilization of sulphur during the burning of organic matter at 575 °C (e.g., Body et al., 2014) did not occur in all studied litters. In contrast, a systematic decrease in leachable phosphate between the 300 and 600 °C ash (by a factor of 5 to 10) is consistent with previous observations on heat-induced conversion of non-available (organic) P into  $\text{PO}_4$  (Carter and Foster, 2004). It is known that, under moderate intensity fires, soils are enriched in the inorganic labile P (Saa et al., 1993, 1994), whereas high intensity burns (above 500 °C) strongly decrease availability of phosphates (Quintana et al., 2007). This, combined with the experimental results of this study, suggests a conversion of the organic P pool into mineral forms at higher temperatures. These phases could be represented by insoluble alkaline-earth elements (Grubb et al., 2000) or Fe and Al phosphates (Vlamis, Gowans, 1961). This is consistent with a sizable increase in the pH of leachates between 300 and 600 °C burned ash, given that metal phosphate solubility decreases with increasing pH (Lindsay, Vlek, 1979; Stumm and Morgan, 1995).

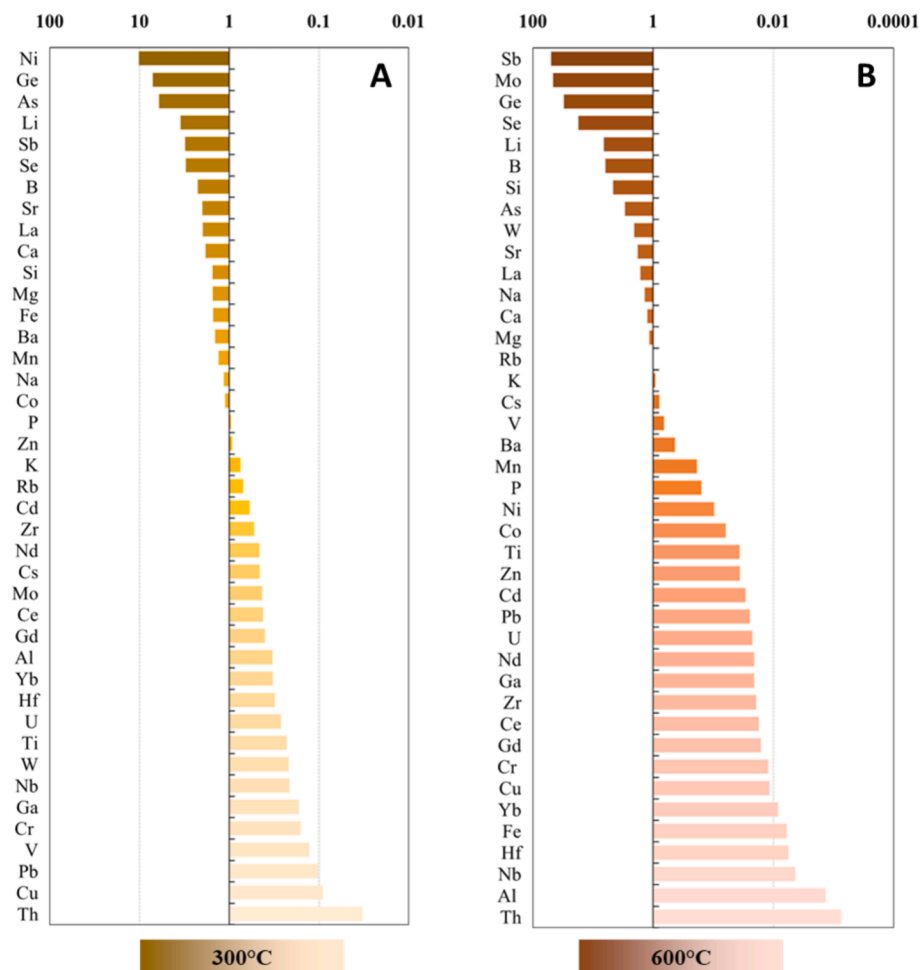


**Fig. 6A,B.** A, B. Ratios of mass normalized solute yield from 300 °C ash to that from fresh litter (yellow, left panel), and from 600 °C ash to that from litter (red, right panel). The mean values of the three MP (the upland, slope and depression) are used for construction of these histograms. (For interpretation of the references to color in this figure legend, the reader is referred to the web version of this article.)

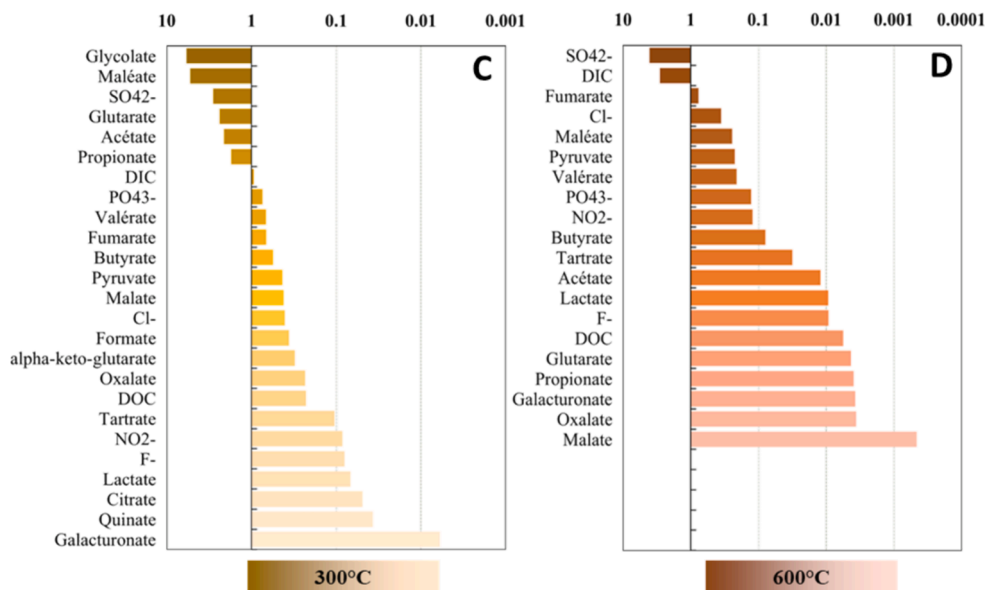


**Fig. 6C,D.** Ratios of mass-normalized solute yield from ash-300 °C to that from fresh litter (yellow, left panel), and from ash-600 °C to that from litter (red, right panel). The mean values of three MP (upland, slope and depression) are used for construction of these histograms. (For interpretation of the references to color in this figure legend, the reader is referred to the web version of this article.)

4.2. Comparison of elementary yield between fresh litter and its ash

A recent study on tundra fire impact demonstrated that, among the three main organic substrates of palsa peatbogs—moss, lichen and peat, the moss ash was by far (by a factor of 2 to 10) more reactive because it yielded the largest changes in solute concentration over first 2 days of reaction time (Kuzmina et al., 2022). The dominance of moss in litter from the depression can partially explain the much higher yield of many organic and inorganic solutes from the ash of this microlandscape observed in the present study. This is also confirmed by mesocosm experiments in natural lake water with ashes and biomass comprised of ground vegetation from permafrost peatlands (Manasygov et al., 2017; Shirokova et al., 2021), which demonstrated a dominance of moss and its ash in DOC and element release into the aqueous solution. Therefore, results of the present study further corroborate previous findings that both moss (a dominant component of litter in the depression) and its ash provide the highest yield of most macro- and micronutrients.

A novel find in this study is the much lower mass normalized yield of

organic and inorganic solutes from ash compared to fresh (unburned) litter (Table 1 and Fig. 7). For the same initial solid: solution ratio, the DOC, carboxylates, many major nutrients (N, P, K) and major cations and anions as well as micronutrients, geochemical tracers and toxicants were enriched by a factor of 3 to 10 in litter leachates compared to ash leachates. A possible reason explaining high reactivity of organic litter compared to ash is less refractory nature of an element which is dispersed in the organic matrices compared to mineral phases of the ash produced after burning. For example, in Central Siberian watersheds, larch litter is capable of delivering the majority of dissolved elements to the river, in the amount comparable to or exceeding the downstream export, on the annual scale (Pokrovsky et al., 2005, 2012). In particular, due to sizable pools of dispersed Ca and Si in the organic matrix of plant biomass, the release rate of these elements from the litter is superior to that from soil-contituent minerals (Frayse et al., 2010).

In contrast to colloidal (3 kDa – 0.45 μm) forms, which dominated most elements in DOM-rich litter leachates, much lower concentrations of DOM in ash leachates allowed for a higher proportion of “truly”

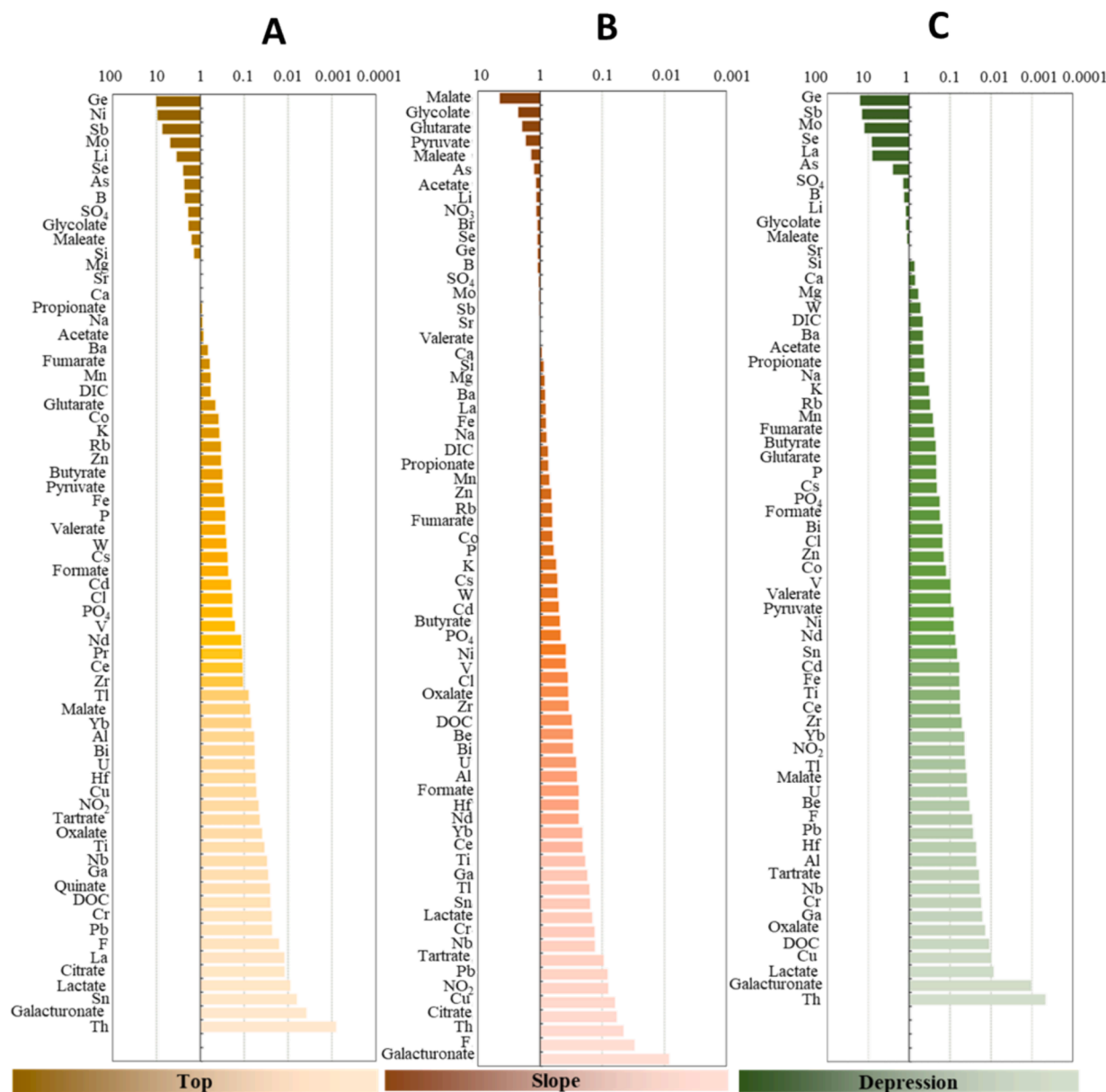


Fig. 7. Ratios of component yield per m<sup>2</sup> of land for unburned (fresh) litter to that of burnt litter (averaged for 3 temperature of ashing), separately for each three MPs. For stock calculation, the field-measured mass of litter per m<sup>2</sup> of land in each site was used. See Table S5 for details.

dissolved low molecular weight (<3 kDa) forms. Indeed, we noted a clear difference in the chemistry of leachates from ash and litter. The majority of elements are present in colloidal form in unburned litter leachates. This difference can be linked to a much higher concentration of colloidal OM and some mineral components (i.e., Fe and Al) in litter leachates. These organic and organo-mineral colloids can bind many trace metals via adsorption onto the surface, coprecipitate with the bulk of Al / Fe hydroxides or form complexes with organic matter, as has been established for surface and soil waters in permafrost peatlands (Pokrovsky et al., 2016; Raudina et al., 2021). Despite the lower amount of colloids in ash leachates, the yield of low molecular weight (LMW<sub>< 3 kDa</sub>), potentially bioavailable fraction from the ash was still lower or comparable to that of fresh litter exempting a few labile elements present in the form of anions or neutral molecules such as Ge, Sb, Se, Mo and W (Fig. S3).

To summarize, considering that *i*) the apparent rate of organic nutrients and major and trace element release from fresh litter is comparable or even faster than that from litter ash and *ii*) the yield of both conventionally dissolved (<0.45 μm) and LMW<sub>< 3 kDa</sub> bioavailable fractions of most nutrients from ash is lower than that from fresh litter, the overall leachability of organic and inorganic nutrients from the litter of each microtopography position is greater than that from the relevant ash.

#### 4.3. Possible implications and limitations of this study

Unlike arid climate regions, where mobilization of ash constituents from soil to surface waters is limited by water availability after a fire event (i.e., Bodi et al., 2014; Certini, 2005; Preston and Schmidt, 2006; Flannigan et al., 2009; Olefeldt et al., 2013; Hauer and Spencer, 1998), the humid climate of western Siberia (with its excess of precipitation over evapotranspiration) and impermeable permafrost layers allow rapid, complete and essentially surface or shallow subsurface export of ash constituents to the adjacent hydrological network (e.g., Parham et al., 2013; Kuzmina et al., 2022). As a result, the fire severity will be the dominant factor controlling the degree of wild fire impact on aquatic environments, compared to soil water residence time and the position of burned sites on the catena. At the same time, the fire severity and intensity can impact the release solutes in a different degree, via generally decreasing the release of organic nutrients and trace metals and increasing the yield from ash of anions and neutral molecules (Table 1, Fig. 5). In contrast to ash, fresh litter demonstrated a much higher capacity to release organic and inorganic nutrients to external aqueous media.

Collectively, results of the present study suggest that, given climate predictions (Ludwig et al., 2018; Novenko et al., 2022) increased frequency, severity, and areal extent of wild fires in northwestern Siberia resulting in removal of organic litter by fire and transformation it into ash will likely decrease the leaching of DOC, organic nutrients (carboxylates), inorganic macro nutrients (N, P, Si, K, Ca and Mg) and most micro-nutrients such as Zn, Ni, Co, Mn, Fe and Mo to soil porewater. Assessment of coupled C and macro-nutrient and micronutrient response to wildfire in the taiga of the discontinuous permafrost subarctic zone will contribute to understanding wild fire impacts on surface water quality and the CO<sub>2</sub> exchange between receiving water bodies and the atmosphere. Results of our experiments suggest that low-severity (smoldering) fires of forest and bog litter produce the ash which is capable releasing the highest amount of macro- and micro-nutrients to the soil porewater.

However, our estimations of ash leaching impact on soil pore water and aquatic ecosystems are highly conservative and subjected to strong uncertainties. Among the factors that were not considered here is the temporal pattern of wildfire. Indeed, the effects of wildfire may be drastically more important at the scale of a single burn event (i.e., Carignan et al., 2000), or immediately after the fire (Granath et al., 2021). Furthermore, we could not assess other physical, chemical and

biological effects of groundfire such as post-fire ecosystem productivity (Amiro et al., 2000; Loranty et al., 2016), organic soil layer disturbances (Gonzalez-Perez et al., 2004; Jiang et al., 2017), CO<sub>2</sub> emissions (Turtsky et al., 2011; Walker et al., 2018), nitrogen cycling (Rodríguez-Cardona et al., 2020; Abbott et al., 2021), microbial activity (Ludwig et al., 2018), particulate emissions and surface albedo change (Jafarov et al., 2013; Loranty et al., 2018). Other limitations of our approach include *(i)* ignoring post-fire hydrology such as runoff-enhanced soil erosion and relevant increase in suspended particulate matter transfer from the soil to the river and *(ii)* elements volatilization and their loss with smoke. Taking into account aforementioned factors is certainly necessary for further assessment of element mass balance at the coupled terrestrial-aquatic ecosystems of permafrost peatlands.

## 5. Conclusions

Laboratory experiments of major organic and inorganic nutrients and trace elements leaching from burnt and fresh litter allowed for identification of first order physico-chemical factors controlling solute yield and indicated a possibility for extrapolating these laboratory findings to natural permafrost-affected forest/peatland ecosystems that are subjected to ground fire. Experiments demonstrated a role of a microtopography position within the catena on element release from the ash, thereby confirming the first hypothesis of this study. The pH and DOC in leachates were largely controlled by the burn temperature of the litter, and thus the yield of DOC, carboxylates and a number of macro- and micronutrients strongly decreased with increased ashing temperature. This generally confirms the second hypothesis of this study, on ashing temperature control on chemical composition of leachates. In accordance with the third hypothesis of this study, aqueous solution acidity and concentration of DOC were two primary factors controlling major and trace element release from ash. Two main group of solutes were identified dependent on their concentration or the mass-normalized yield from ash prepared at different temperatures. Solute of the first group (organic nutrients such as DOC and carboxylic acids), phosphate, metal micronutrients, toxic metals and low-mobility trace elements strongly decreased their concentration in leachates with increases in ashing temperature. Solute of the second group (labile, soluble major and trace elements present as anions or neutral molecules, alkalis and alkaline-earth metals) either increased (by a factor of 2 to 3) or remained indifferent to ashing temperatures. Correlations between different solutes in ash and fresh litter leachates revealed DOC and Fe as main carriers of trace metals and micronutrients, essentially in the colloidal form.

The mass-normalized release of the majority of organic and inorganic macro- and micronutrients from fresh (unburned) litter was up to an order of magnitude higher than that from litter ash, regardless of the microtopography position. Furthermore, the capacity of ash to deliver most bioavailable low molecular weight (<3 kDa) forms of inorganic nutrients is not higher than that of fresh litter. The broad significance of this experimental finding is that the impact of forest-tundra fire on carbon, nutrient and major and trace element release from ash to soil solution will be strongly dependent on fire severity and in a lesser degree on microtopographic position on the soil catena.

### CRedit authorship contribution statement

**Daria Kuzmina:** Writing – original draft, Investigation, Data curation. **Sergey V. Loiko:** Methodology, Data curation, Conceptualization. **Artem G. Lim:** . **Georgy I. Istigechev:** Visualization, Data curation. **Sergey P. Kulizhsky:** Resources, Project administration, Funding acquisition. **Frederic Julien:** Methodology, Investigation. **Jean-Luc Rols:** Investigation, Manuscript editing. **Oleg S. Pokrovsky:** Writing – original draft, Formal analysis.

## Declaration of competing interest

The authors declare that they have no known competing financial interests or personal relationships that could have appeared to influence the work reported in this paper.

## Data availability

All the primary data on major and trace solute leachates from ash and litter are available at the Mendeley Database: Kuzmina, Daria; Lim, Artyom; Pokrovsky, Oleg (2023), "Experimental yields of major and trace solute in aqueous leachates of ash and plant litter from permafrost peatland", Mendeley Data, V1, doi: 10.17632/dxhgsmvhwm.1.

## Acknowledgements

The study was funded by the RSF grant No 23-17-00281, and the TSU Development Program "Priority-2030". OP is grateful for partial support from PEPR "PEACE" (ANR-22- PEXF-0011). Chris Benker is thanked for English editing.

## Appendix A. Supplementary data

Supplementary data to this article can be found online at <https://doi.org/10.1016/j.geoderma.2024.116925>.

## References

- Abakumov, E., Pechkin, A., Chebykina (Maksimova), E., Shamilishvili, G., 2020. Effect of the wildfires on sandy podzol soils of Nadym region, Yamalo-Nenets autonomous district, Russia. *Appl. Environ. Soil Sci.* 2020, e8846005.
- Abbott, B.W., Rocha, A.V., Shogren, A., Zarnetske, J.P., Iannucci, F., Bowden, W.B., Bratsman, S.P., Patch, L., Watts, R., Fulweber, R., Frei, R.J., Huebner, A.M., Ludwig, S.M., Carling, G.T., O'Donnell, J.A., 2021. Tundra wildfire triggers sustained lateral nutrient loss in Alaskan Arctic. *Glob. Change Biol.* 27, 1408–1430. <https://doi.org/10.1111/gcb.15507>.
- Ackley, C., Tank, S.E., Haynes, K.M., Rezaneshad, F., McCarter, C., Quinton, W.L., 2021. Coupled hydrological and geochemical impacts of wildfire in peatland-dominated regions of discontinuous permafrost. *Sci. Total Environ.* 782, 146841 <https://doi.org/10.1016/j.scitotenv.2021.146841>.
- Agafontsev, N.V., Kasymov, D.P., 2020. Estimation of the parameters of combustion of the surface of natural combustible materials by the thermography method. *J. Eng. Phys. Thermophys.* 93, 998–1003. <https://doi.org/10.1007/s10891-020-02200-w>.
- Amiro, B.D., Chen, J.M., Liu, J., 2000. Net primary productivity following forest fire for Canadian ecoregions. *Can. J. For. Res.* 30, 939–947. <https://doi.org/10.1139/x00-025>.
- Basso, M., Vieira, D.C.S., Ramos, T.B., Mateus, M., 2020. Assessing the adequacy of SWAT model to simulate postfire effects on the watershed hydrological regime and water quality. *Land Degrad. Dev.* 31, 619–631.
- Beilman, D.W., MacDonald, G.M., Smith, L.C., Reimer, P.J., 2009. Carbon accumulation in peatlands of West Siberia over the last 2000 years. *Glob. Biogeochem. Cycles* 23, GB1012. <https://doi.org/10.1029/2007GB003112>.
- Benscoter, B.W., Thompson, D.K., Waddington, J.M., Flannigan, M.D., Wotton, B.M., de Groot, W.J., Turetsky, M.R., Benscoter, B.W., Thompson, D.K., Waddington, J.M., Flannigan, M.D., Wotton, B.M., de Groot, W.J., Turetsky, M.R., 2011. Interactive effects of vegetation, soil moisture and bulk density on depth of burning of thick organic soils. *Int. J. Wildland Fire* 20, 418–429. <https://doi.org/10.1071/WF08183>.
- Betts, E.F., Jones Jr., J.B., 2009. Impact of wildfire on stream nutrient chemistry and ecosystem metabolism in boreal forest catchments of Interior Alaska. *Arctic, Antarctic, and Alpine Research* 41 (4), 407–417. <https://doi.org/10.1657/1938-4246-41.4.407>.
- Bodí, M.B., Martín, D.A., Balfour, V.N., Santín, C., Doerr, S.H., Pereira, P., Cerdà, A., Mataix-Solera, J., 2014. Wildland fire ash: production, composition and eco-hydro-geomorphic effects. *Earth-Sci. Rev.* 130, 103–127. <https://doi.org/10.1016/j.earscirev.2013.12.007>.
- Botch, M.S., Kobak, K.I., Vinson, T.S., Kolchugina, T.P., 1995. Carbon pools and accumulation in peatlands of the former Soviet Union. *Glob. Biogeochem. Cycles* 9, 37–46. <https://doi.org/10.1029/94GB03156>.
- Burd, K., Tank, S.E., Dion, N., Quinton, W.L., Spence, C., Tanentzap, A.J., Olefeldt, D., 2018. Seasonal shifts in export of DOC and nutrients from burned and unburned peatland-rich catchments, Northwest Territories, Canada. *Hydro. Earth Syst. Sci.* 22, 4455–4472. <https://doi.org/10.5194/hess-2018-253>.
- Burke, J.M., Prepas, E.E., Pinder, S., 2005. Runoff and phosphorus export patterns in large forested watersheds on the western Canadian Boreal Plain before and for 4 years after wildfire. *J. Environ. Eng. Sci.* 4, 319–325. <https://doi.org/10.1139/s04-072>.
- Carignan, R., D'Arcy, P., Lamontagne, S., 2000. Comparative impacts of fire and forest harvesting on water quality in Boreal Shield lakes. *Can. J. Fish. Aquat. Sci.* 57, 105–117. <https://doi.org/10.1139/f00-125>.
- Carter, M.C., Darwin Foster, C., 2004. Prescribed burning and productivity in southern pine forests: a review. *For. Ecol. Manag.* 191, 93–109. <https://doi.org/10.1016/j.foreco.2003.11.006>.
- Certini, G., 2005. Effects of fire on properties of forest soils: A review. *Oecologia* 143, 1–10. <https://doi.org/10.1007/s00442-004-1788-8>.
- Chen, Y., Hu, F.S., Lara, M.J., 2021. Divergent shrub-cover responses driven by climate, wildfire, and permafrost interactions in Arctic tundra ecosystems. *Glob. Change Biol.* 27, 652–663. <https://doi.org/10.1111/gcb.15451>.
- Christensen, N.L., 1973. Fire and the nitrogen cycle in California Chaparral. *Science* 181, 66–68. <https://doi.org/10.1126/science.181.4094.66>.
- Crandall T., et al. 2021. Megafire affects stream sediment flux and dissolved organic matter reactivity, but land use dominates nutrient dynamics in semiarid watersheds. *PLoS One*, 16 Art No e0257733.
- Czimczik, C.I., Preston, C.M., Schmidt, M.W.I., Schulze, E.-D., 2003. How surface fire in Siberian Scots pine forests affects soil organic carbon in the forest floor: Stocks, molecular structure, and conversion to black carbon (charcoal). *Glob. Biogeochem. Cycles* 17, 1020. <https://doi.org/10.1029/2002GB001956>.
- Delplace, G., Schreck, E., Pokrovsky, O.S., Zouiten, C., Blondet, I., Darrozes, J., et al., 2020. Accumulation of heavy metals in phytoliths from reeds growing on mining environments in southern Europe. *Sci. Total Environ.* 712. Art No 135595.
- Diemer, L.A., McDowell, W.H., Wymore, A.S., Prokushkin, A.S., 2015. Nutrient uptake along a fire gradient in boreal streams of Central Siberia. *Freshwater Sci.* 34, 1443–1456. <https://doi.org/10.1086/683481>.
- Filkov, A.I., Tihay-Fellicelli, V., Masoudvaziri, N., Rush, D., Valencia, A., Wang, Y., Blunck, D.L., Valero, M.M., Kempna, K., Smolka, J., De Beer, J., Campbell-Lochrie, Z., Centeno, F.R., Ibrahim, M.A., Lemmert, K.C., Tam, W.C., 2023. A review of thermal exposure and fire spread mechanisms in large outdoor fires and the built environment. *Fire Safety J.* 140, Art No 103871. <https://doi.org/10.1016/j.firesaf.2023.103871>.
- Flannigan, M.D., Stocks, B.J., Wotton, B.M., 2000. Climate change and forest fires. *Sci. Total Environ.* 262, 221–229. [https://doi.org/10.1016/S0048-9697\(00\)00524-6](https://doi.org/10.1016/S0048-9697(00)00524-6).
- Flannigan, M., Stocks, B., Turetsky, M., Wotton, M., 2009. Impacts of climate change on fire activity and fire management in the circumboreal forest. *Glob. Change Biol.* 15, 549–560. <https://doi.org/10.1111/j.1365-2486.2008.01660.x>.
- Frayse, F., Pokrovsky, O.S., Meunier, J.-D., 2010. Experimental study of terrestrial plant litter interaction with aqueous solutions. *Geochim. Cosmochim. Acta* 74, 70–84.
- Gao, C., Wang, G., Cong, J., Freeman, C., Jiang, M., Qin, L., 2023. High intensity fire accelerates accumulation of a stable carbon pool in permafrost peatlands under climate warming. *Catena*, 227 Art No 107108, <https://doi.org/10.1016/j.catena.2023.107108>.
- Gibson, C.M., Chasmer, L.E., Thompson, D.K., Quinton, W.L., Flannigan, M.D., Olefeldt, D., 2018. Wildfire as a major driver of recent permafrost thaw in boreal peatlands. *Nat. Commun.* 9, 3041. <https://doi.org/10.1038/s41467-018-05457-1>.
- Giesler, R., Lundström, U., 1993. Soil solution chemistry: Effects of bulking soil samples. *Soil Sci. Soc. Amer. J.* 57, 1283–1288. <https://doi.org/10.2136/sssaj1993.03615995005700050020x>.
- González-Pérez, J.A., González-Vila, F.J., Almendros, G., Knicker, H., 2004. The effect of fire on soil organic matter - A review. *Environ. Int.* 30, 855–870. <https://doi.org/10.1016/j.envint.2004.02.003>.
- Goryachkin, S.V., 2010. Soil cover of the north: structure, genesis, ecology, and evolution. GEOS, Moscow (In Russian).
- Granath, G., Evans, C.D., Strengbom, J., Fölster, J., Grelle, A., Strömquist, J., Köhler, S.J., 2021. The impact of wildfire on biogeochemical fluxes and water quality in boreal catchments. *Biogeosciences* 18, 3243–3261. <https://doi.org/10.5194/bg-18-3243-2021>.
- Gray, D.M., Dighton, J., 2006. Mineralization of forest litter nutrients by heat and combustion. *Soil Biol. Biochem.* 38, 1469–1477. <https://doi.org/10.1016/j.soilbio.2005.11.003>.
- Grier, C.C., 1975. Wildfire effects on nutrient distribution and leaching in a coniferous ecosystem. *Can. J. For. Res.* 5, 599–607. <https://doi.org/10.1139/x75-087>.
- Grubb, D.G., Guimaraes, M.S., Valencia, R., 2000. Phosphate immobilization using an acidic type F fly ash. *J. Hazard. Mater.* 76, 217–236. [https://doi.org/10.1016/S0304-3894\(00\)0200-4](https://doi.org/10.1016/S0304-3894(00)0200-4).
- Gustafsson, J. Visual MINTEQ ver. 3.1. <http://vminetq.lwr.kth.se>, 2014, assessed 8.02.2020.
- Hampton, T.B., Lin, S., Basu, N.B., 2022. Forest fire effects on stream water quality at continental scales: a meta-analysis. *Environ. Res. Lett.* 17, 064003 <https://doi.org/10.1088/1748-9326/ac6a6c>.
- Harden, J.W., Neff, J.C., Sandberg, D.V., Turetsky, M.R., Ottmar, R., Gleixner, G., Fries, T.L., Manies, K.L., 2004. Chemistry of burning the forest floor during the FROSTFIRE experimental burn, interior Alaska, 1999. *Glob. Biogeochem. Cycles* 18, GD3014. <https://doi.org/10.1029/2003GB002194>.
- Hauer, F.R., Spencer, C.N., 1998. Phosphorus and nitrogen dynamics in streams associated with wildfire: a study of immediate and longterm effects. *Int. J. Wildland Fire* 8, 183–198. <https://doi.org/10.1071/wf980183>.
- Heim, R.J., Yurtaev, A., Bucharova, A., Heim, W., Kutsir, V., Knorr, K.-H., Lampei, C., Pechkin, A., Schilling, D., Sulkarnaev, F., Hölzel, N., 2022. Fire in lichen-rich subarctic tundra changes carbon and nitrogen cycling between ecosystem compartments but has minor effects on stocks. *Biogeosciences* 19, 2729–2740. <https://doi.org/10.5194/bg-19-2729-2022>.
- Hrelja, I., Šestak, I., Delač, D., Pereira, P., Bogunović, I., 2022. Soil chemical properties and trace elements after wildfire in mediterranean Croatia: effect of severity,

- vegetation type and time-since-fire. *Agronomy* 12, 1515. <https://doi.org/10.3390/agronomy12071515>.
- Hu, F.S., Higuera, P.E., Duffy, P., Chipman, M.L., Rocha, A.V., Young, A.M., Kelly, R., Dietz, M.C., 2015. Arctic tundra fires: natural variability and responses to climate change. *Front. Ecol. Environ.* 13, 369–377. <https://doi.org/10.1890/1500663>.
- Jafarov, E.E., Romanovsky, V.E., Genet, H., McGuire, A.D., Marchenko, S.S., 2013. The effects of fire on the thermal stability of permafrost in lowland and upland black spruce forests of interior Alaska in a changing climate. *Environ. Res. Lett.* 8, 035030 <https://doi.org/10.1088/1748-9326/8/3/035030>.
- Jiang, Y., Rastetter, E.B., Shaver, G.R., Rocha, A.V., Zhuang, Q., Kwiatkowski, B.L., 2017. Modeling long-term changes in tundra carbon balance following wildfire, climate change, and potential nutrient addition. *Ecol. Appl.* 27, 105–117. <https://doi.org/10.1002/eap.1413>.
- Kasischke, E.S., Hyer, E.J., Novelli, P.C., Bruhwiler, L.P., French, N.H.F., Sukhinin, A.I., Hewson, J.H., Stocks, B.J., 2005. Influences of boreal fire emissions on Northern Hemisphere atmospheric carbon and carbon monoxide. *Glob. Biogeochem. Cycles* 19, GB1012. <https://doi.org/10.1029/2004GB002300>.
- Kasischke, E.S., Turetsky, M.R., 2006. Recent changes in the fire regime across the North American boreal region—Spatial and temporal patterns of burning across Canada and Alaska. *Geophys. Res. Lett.* 33, G04016. <https://doi.org/10.1029/2006GL025677>.
- Kasischke, E.S., Verbyla, D.L., Rupp, T.S., McGuire, A.D., Murphy, K.A., Jandt, R., Barnes, J.L., Hoy, E.E., Duffy, P.A., Calef, M., Turetsky, M.R., 2010. Alaska's changing fire regime — implications for the vulnerability of its boreal forests. *Can. J. for. Res.* 40, 1313–1324. <https://doi.org/10.1139/X10-098>.
- Kauffman, J.B., Sanford Jr., R.L., Cummings, D.L., Salcedo, I.H., Sampaio, E.V.S.B., 1993. Biomass and nutrient dynamics associated with slash fires in neotropical dry forests. *Ecology* 74, 140–151. <https://doi.org/10.2307/1939509>.
- Kawahigashi, M., Prokushkin, A., Sumida, H., 2011. Effect of fire on solute release from organic horizons under larch forest in Central Siberian permafrost terrain. *Geoderma* 166, 171–180. <https://doi.org/10.1016/j.geoderma.2011.07.027>.
- Kharuk, V.I., Ponomarev, E.I., Ivanova, G.A., Dvinskaya, M.L., Coogan, S.C.P., Flannigan, M.D., 2021. Wildfires in the Siberian taiga. *Ambio* 50, 1953–1974. <https://doi.org/10.1007/s13280-020-01490-x>.
- Knorre, A.A., Kirdyanov, A.V., Prokushkin, A.S., Krusic, P.J., Büntgen, U., 2019. Tree ring-based reconstruction of the long-term influence of wildfires on permafrost active layer dynamics in Central Siberia. *Sci. Total Environ.* 652, 314–319. <https://doi.org/10.1016/j.scitotenv.2018.10.124>.
- Koyama, A., Kavanagh, K.L., Stephan, K., 2010. Wildfire effects on soil gross nitrogen transformation rates in coniferous forests of central Idaho, USA. *Ecosystems* 13, 1112–1126. <https://doi.org/10.1007/s10021-010-9377-7>.
- Kuzmina, D., Lim, A.G., Loiko, S.V., Pokrovsky, O.S., 2022. Experimental assessment of tundra fire impact on element export and storage in permafrost peatlands. *Sci. Total Environ.* 853, 158701 <https://doi.org/10.1016/j.scitotenv.2022.158701>.
- Kuzmina, D.M., Lim, A.G., Loiko, S.V., Shefer, N., Shirokova, L.S., Julien, F., Rols, J.-L., Pokrovsky, O.S., 2023. Dispersed ice of permafrost peatlands represents an important source of labile carboxylic acids, nutrients and metals. *Geoderma* 429, 116256. <https://doi.org/10.1016/j.geoderma.2022.116256>.
- Lea, P.D., Waythomas, C.F., 1990. Late-pleistocene eolian sand sheets in Alaska. *Quat. Res.* 34, 269–281. [https://doi.org/10.1016/0033-5894\(90\)90040-R](https://doi.org/10.1016/0033-5894(90)90040-R).
- Liljedahl, A., Hinzman, L., Busey, R., Yoshikawa, K., 2007. Physical short-term changes after a tussock tundra fire, Seward Peninsula, Alaska. *J. Geophys. Res. Earth Surf.* 112, F02S07. <https://doi.org/10.1029/2006JF000554>.
- Lim, A.G., Loiko, S.V., Kuzmina, D.M., Krickov, I.V., Shirokova, L.S., Kulizhsky, S.P., Pokrovsky, O.S., 2022. Organic carbon, and major and trace elements reside in labile low-molecular form in the ground ice of permafrost peatlands: a case study of colloids in peat ice of Western Siberia. *Environ. Sci. Process. Impacts* 24, 1443. <https://doi.org/10.1039/D1EM00547B>.
- Lindsay, W.L., Vlek, P.L.G., Chien, S.H., 1989. Phosphate Minerals, in: *Minerals in Soil Environments*. John Wiley & Sons, Ltd, pp. 1089–1130. <https://doi.org/10.2136/sssabookser1.2ed.c22>.
- Liu, H., Zak, D., Zableckis, N., Gossmer, A., Langhammer, N., Meermann, B., Lennartz, B., 2023. Water pollution risks by smoldering fires in degraded peatlands. *Sci. Total Environ.* 871, Art No 161979.
- Loiko, S.V., Kuz'mina, D.M., Dudko, A.A., Konstantinov, A.O., Vasil'eva, Yu.A., Kurasova, A.O., Lim, A.G., Kulizhskii, S.P., 2022. Charcoals in the middle taiga podzols of Western Siberia as an indicator of geosystem history. *Eurasian Soil Sci.* 55, 154–168. <https://doi.org/10.1134/S1064229322020089>.
- Loranty, M.M., Lieberman-Cribbin, W., Berner, L.T., Natali, S.M., Goetz, S.J., Alexander, H.D., Kholodov, A.L., 2016. Spatial variation in vegetation productivity trends, fire disturbance, and soil carbon across arctic-boreal permafrost ecosystems. *Environ. Res. Lett.* 11, 095008 <https://doi.org/10.1088/1748-9326/11/9/095008>.
- Loranty, M.M., Abbott, B.W., Blok, D., Douglas, T.A., Epstein, H.E., Forbes, B.C., Jones, B. M., Kholodov, A.L., Kropp, H., Malhotra, A., Mamet, S.D., Myers-Smith, I.H., Natali, S.M., O'Donnell, J.A., Phoenix, G.K., Rocha, A.V., Sonnentag, O., Tape, K.D., Walker, D.A., 2018. Reviews and syntheses: Changing ecosystem influences on soil thermal regimes in northern high-latitude permafrost regions. *Biogeosciences* 15, 5287–5313. <https://doi.org/10.5194/bg-15-5287-2018>.
- Ludwig, S.M., Alexander, H.D., Kielland, K., Mann, P.J., Natali, S.M., Ruess, R.W., 2018. Fire severity effects on soil carbon and nutrients and microbial processes in a Siberian larch forest. *Glob. Change Biol.* 24, 5841–5852. <https://doi.org/10.1111/gcb.14455>.
- Manaspov, R.M., Shirokova, L.S., Pokrovsky, O.S., 2017. Experimental modeling of thaw lake water evolution in discontinuous permafrost zone: Role of peat, lichen leaching and ground fire. *Sci. Total Environ.* 580, 245–257. <https://doi.org/10.1016/j.scitotenv.2016.12.067>.
- Mann, D.H., Heiser, P.A., Finney, B.P., 2002. Holocene history of the Great Kobuk Sand Dunes, Northwestern Alaska. *Quat. Sci. Rev.* 21, 709–731. [https://doi.org/10.1016/S0277-3791\(01\)00120-2](https://doi.org/10.1016/S0277-3791(01)00120-2).
- Marcotte, A.L., Limpens, J., Stooft, C.R., Stoorvogel, J.J., 2022. Can ash from smoldering fires increase peatland soil pH? *Int. J. Wildland Fire* 31 (6), 607–620.
- Masyagina, O.V., Tokareva, I.V., Prokushkin, A.S., 2016. Post fire organic matter biodegradation in permafrost soils: Case study after experimental heating of mineral horizons. *Sci. Total Environ.* 573, 1255–1264. <https://doi.org/10.1016/j.scitotenv.2016.04.195>.
- McCullough, I.M., Cheruvellil, K.S., Lapierre, J.-F., Lottig, N.R., Moritz, M.A., Stachelek, J., Soranno, P.A., 2019. Do lakes feel the burn? Ecological consequences of increasing exposure of lakes to fire in the continental United States *Glob. Change Biol.* 25, 2841–2854.
- Mergelov, N., Petrov, D., Zazovskaya, E., Dolgikh, A., Golyeva, A., Matskovsky, V., Bichurin, R., Turchinskaya, S., Belyaev, V., Goryachkin, S., 2020. Soils in karst sinkholes record the holocene history of local forest fires at the north of European Russia. *Forests* 11, 1268. <https://doi.org/10.3390/f11121268>.
- Miner, K.R., Turetsky, M.R., Malina, E., Bartsch, A., Tamminen, J., McGuire, A.D., Fix, A., Sweeney, C., Elder, C.D., Miller, C.E., 2022. Permafrost carbon emissions in a changing Arctic. *Nat. Rev. Earth Environ.* 3, 55–67. <https://doi.org/10.1038/s43017-021-00230-3>.
- Mishra, A., Alnahit, A., Campbell, B., 2021. Impact of land uses, drought, flood, wildfire, and cascading events on water quality and microbial communities: a review and analysis. *J. Hydrol.* 596, Art No 125707.
- Moilanen, M., Silfverberg, K., Hokkanen, T.J., 2002. Effects of wood-ash on the tree growth, vegetation and substrate quality of a drained mire: a case study. *For. Ecol. Manag.* 171, 321–338. [https://doi.org/10.1016/S0378-1127\(01\)00789-7](https://doi.org/10.1016/S0378-1127(01)00789-7).
- Neff, J.C., Harden, J.W., Gleixner, G., 2005. Fire effects on soil organic matter content, composition, and nutrients in boreal interior Alaska. *Can. J. for. Res.* 35, 2178–2187. <https://doi.org/10.1139/x05-154>.
- Nelson, K., Thompson, D., Hopkinson, C., Petrone, R., Chasmer, I., 2021. Peatland-fire interactions: a review of wildland fire feedbacks and interactions in Canadian boreal peatlands. *Sci. Total Environ.* 769, Art No 145212.
- Novenko, E.Y., Kupryanov, D.A., Mazei, N.G., Prokushkin, A.S., Phelps, L.N., Buri, A., Davis, B.A.S., 2022. Evidence that modern fires may be unprecedented during the last 3400 years in permafrost zone of Central Siberia, Russia. *Environ. Res. Lett.* 17, 025004 <https://doi.org/10.1088/1748-9326/ac4b53>.
- Olefeldt, D., Turetsky, M.R., Blodau, C., 2013. Altered composition and microbial versus UV-mediated degradation of dissolved organic matter in boreal soils following wildfire. *Ecosystems* 16, 1396–1412. <https://doi.org/10.1007/s10021-013-9691-y>.
- Parham, L.M., Prokushkin, A.S., Pokrovsky, O.S., Titov, S.V., Grekova, E., Shirokova, L. S., McDowell, W.H., 2013. Permafrost and fire as regulators of stream chemistry in basins of the Central Siberian Plateau. *Biogeochemistry* 116, 55–68. <https://doi.org/10.1007/s10533-013-9922-5>.
- Pereira, P., Úbeda, X., Martín, D.A., 2012. Fire severity effects on ash chemical composition and water-extractable elements. *Geoderma, Fire Effects on Soil Properties* 191, 105–114. <https://doi.org/10.1016/j.geoderma.2012.02.005>.
- Pereira, P., Úbeda, X., Martín, D., Mataix-Solera, J., Cerdà, A., Burguet, M., 2014. Wildfire effects on extractable elements in ash from a Pinus pinaster forest in Portugal. *Hydrol. Process.* 28, 3681–3690. <https://doi.org/10.1002/hyp.9707>.
- Pereira, P., Cerdà, A., Martín, D., Úbeda, X., Depelgrin, D., Novara, A., Martínez-Murillo, J.F., Brevik, E.C., Menshov, O., Comino, J.R., Miesel, J., 2017. Short-term low-severity spring grassland fire impacts on soil extractable elements and soil ratios in Lithuania. *Sci. Total Environ.* 578, 469–475. <https://doi.org/10.1016/j.scitotenv.2016.10.210>.
- Petrone, K.C., Hinzman, L.D., Shibata, H., Jones, J.B., Boone, R.D., 2007. The influence of fire and permafrost on sub-arctic stream chemistry during storms. *Hydrol. Process.* 21, 423–434. <https://doi.org/10.1002/hyp.6247>.
- Pokrovsky, O.S., Schott, J., Kudryavtzev, D.I., Dupré, B., 2005. Basalt weathering in Central Siberia under permafrost conditions. *Geochim. Cosmochim. Acta* 69, 5659–5680. <https://doi.org/10.1016/j.gca.2005.07.018>.
- Pokrovsky, O.S., Viers, J., Dupré, B., Chabaux, F., Gaillardet, J., Audry, S., Prokushkin, A. S., Shirokova, L.S., Kirpotin, S.N., Lapitsky, S.A., Shevchenko, V.P., 2012. Biogeochemistry of carbon, major and trace elements in watersheds of Northern Eurasia drained to the Arctic Ocean: The change of fluxes, sources and mechanisms under the climate warming prospective. *C.R. Geoscience* 344, 663–677.
- Pokrovsky, O.S., Manaspov, R.M., Loiko, S.V., Shirokova, L.S., 2016. Organic and organo-mineral colloids in discontinuous permafrost zone. *Geochim. Cosmochim. Acta* 188, 1–20. <https://doi.org/10.1016/j.gca.2016.05.035>.
- Potter, S., Cooperdock, S., Veraverbeke, S., Walker, X., Mack, M.C., Goetz, S.J., Baltzer, J., Bourgeau-Chavez, L., Burrell, A., Dieleman, C., French, N., Hantson, S., Hoy, E.E., Jenkins, L., Johnstone, J.F., Kane, E.S., Natali, S.M., Randerson, J.T., Turetsky, M.R., Whitman, E., Wiggins, E., Rogers, B.M., 2023. Burned area and carbon emissions across northwestern boreal North America from 2001–2019. *Biogeosciences* 20, 2785–2804. <https://doi.org/10.5194/bg-20-2785-2023>.
- Preston, C.M., Schmidt, M.W.I., 2006. Black (pyrogenic) carbon: a synthesis of current knowledge and uncertainties with special consideration of boreal regions. *Biogeosciences* 3, 397–420. <https://doi.org/10.5194/bg-3-397-2006>.
- Quintana, J.R., Cala, V., Moreno, A.M., Parra, J.G., 2007. Effect of heating on mineral components of the soil organic horizon from a Spanish juniper (*Juniperus thurifera* L.) woodland. *J. Arid Environ.* 71, 45–56. <https://doi.org/10.1016/j.jaridenv.2007.03.002>.
- Raudina, T., Loiko, S.V., Lim, A.G., Manaspov, R.M., Shirokova, L.S., Istigechev, G.I., Kuzmina, D.M., Kulizhsky, S.P., Vorobyev, S.N., Pokrovsky, O.S., 2018. Permafrost thaw and climate warming may decrease the CO<sub>2</sub>, carbon, and metal concentration



- in peat soil waters of the Western Siberia Lowland. *Science Total Environment* 634, 1004–1023.
- Raudina, T.V., Loiko, S.V., Kuzmina, D.M., Shirokova, L.S., Kulizhskiy, S.P., Golovatskaya, E.A., Pokrovsky, O.S., 2021. Colloidal organic carbon and trace elements in peat porewaters across a permafrost gradient in Western Siberia. *Geoderma* 390, 114971. <https://doi.org/10.1016/j.geoderma.2021.114971>.
- Rodríguez-Cardona, B.M., Wymore, A.S., McDowell, W.H., Coble, A.A., Kolosov, R., Prokushkin, A.S., Podgorski, D.C., Zito, P., Spencer, R.G.M., 2020. Wildfires lead to decreased carbon and increased nitrogen concentrations in upland arctic streams. *Sci. Rep.* 10, 1–9. <https://doi.org/10.1038/s41598-020-65520-0>.
- Rust, A.J., Saxe, S., McCray, J.E., Rhoades, C.C., Hogue, T.S., 2019. Evaluating the factors responsible for post-fire water quality response in forests of the western USA. *Int. J. Wildland Fire*, 28 Art No 769.
- Saa, A., Trasar-Cepeda, M.C., Gil-Sotres, F., Carballas, T., 1993. Changes in soil phosphorus and acid phosphatase activity immediately following forest fires. *Soil Biol. Biochem.* 25, 1223–1230. [https://doi.org/10.1016/0038-0717\(93\)90218-Z](https://doi.org/10.1016/0038-0717(93)90218-Z).
- Saá, A., Trasar-Cepeda, M.C., Soto, B., Gil-Sotres, F., Díaz-Fierros, F., 1994. Forms of phosphorus in sediments eroded from burnt soils. *J. Environ. Qual.* 23, 739–746. <https://doi.org/10.2134/jeq1994.00472425002300040018x>.
- Santfín, C., Doerr, S.H., Merino, A., Bryant, R., Loader, N.J., 2016. Forest floor chemical transformations in a boreal forest fire and their correlations with temperature and heating duration. *Geoderma* 264, 71–80. <https://doi.org/10.1016/j.geoderma.2015.09.021>.
- Shirokova, L.S., Chupakov, A.V., Ivanova, I.S., Moreva, O.Y., Zabelina, S.A., Shutskiy, N. A., Loiko, S.V., Pokrovsky, O.S., 2021. Lichen, moss and peat control of C, nutrient and trace metal regime in lakes of permafrost peatlands. *Sci. Total Environ.* 782, 146737 <https://doi.org/10.1016/j.scitotenv.2021.146737>.
- Spencer, C.N., Gabel, K.O., Hauer, F.R., 2003. Wildfire effects on stream food webs and nutrient dynamics in Glacier National Park. *USA. for. Ecol. Manag.* 178, 141–153. [https://doi.org/10.1016/S0378-1127\(03\)00058-6](https://doi.org/10.1016/S0378-1127(03)00058-6).
- Stumm, W., Morgan, J.J., 1995. *Aquatic chemistry: chemical equilibria and rates in natural waters*. John Wiley & Sons, New York.
- Talucci, A.C., Lorant, M.M., Alexander, H.D., 2022. Siberian taiga and tundra fire regimes from 2001–2020. *Environ. Res. Lett.* 17, 025001 <https://doi.org/10.1088/1748-9326/ac3f07>.
- Thomas, J.C., Mueller, E.V., Gallagher, M.R., Clark, K.L., Skowronski, N., Simeoni, A., Hadden, R.M., 2021. Coupled assessment of fire behavior and firebrand dynamics. *Front. Mech. Eng* 7, Art No 650580. <https://doi.org/10.3389/fmech.2021.650580>.
- Turetsky, M.R., Kane, E.S., Harden, J.W., Ottmar, R.D., Manies, K.L., Hoy, E., Kasischke, E.S., 2011. Recent acceleration of biomass burning and carbon losses in Alaskan forests and peatlands. *Nat. Geosci.* 4, 27–31. <https://doi.org/10.1038/ngeo1027>.
- Úbeda, X., Pereira, P., Outeiro, L., Martin, D.A., 2009. Effects of fire temperature on the physical and chemical characteristics of the ash from two plots of cork oak (*Quercus suber*). *Land Degrad. Dev.* 20, 589–608. <https://doi.org/10.1002/ldr.930>.
- Velichko, A.A., Timireva, S.N., Kremenetski, K.V., MacDonald, G.M., Smith, L.C., 2011. West Siberian Plain as a late glacial desert. *Quat. Int.* 237, 45–53. <https://doi.org/10.1016/j.quaint.2011.01.013>.
- Vlams, J., Gowans, K.D., 1961. Availability of nitrogen, phosphorus and sulfur after brush burning. *J. Range Manag.* 14, 38–40. <https://doi.org/10.2307/3894829>.
- Volkova, I.I., Volkov, I.V., Morozova, Y.A., Nikitkin, V.A., Vishnyakova, E.K., Mironycheva-Tokareva, N.P., 2023. Water holding capacity of some bryophyta species from tundra and north taiga of the West Siberia. *Water* 15, Art No 2626. <https://doi.org/10.3390/w15142626>.
- Walker, X.J., Rogers, B.M., Baltzer, J.L., Cumming, S.G., Day, N.J., Goetz, S.J., Johnstone, J.F., Schuur, E.A.G., Turetsky, M.R., Mack, M.C., 2018. Cross-scale controls on carbon emissions from boreal forest megafires. *Glob. Change Biol.* 24, 4251–4265. <https://doi.org/10.1111/gcb.14287>.
- Whelan, R.J., 1995. *The Ecology of Fire*. Cambridge University Press, New York.
- White, E.M., Thompson, W.W., Gartner, F.R., 1973. Heat effects on nutrient release from soils under ponderosa pine. *J. Range Manag.* 26, 22–24. <https://doi.org/10.2307/3896875>.
- Wu, Y., Xu, X., McCarter, C.P.R., Zhang, N., Ganzoury, M.A., Waddington, J.M., de Lannoy, C.-F., 2022. Assessing leached TOC, nutrients and phenols from peatland soils after lab-simulated wildfires: Implications to source water protection. *Sci. Total Environ.* 822, Art No 153579 <https://doi.org/10.1016/j.scitotenv.2022.153579>.
- Yeghicheyan, D., Aubert, D., Bouhnik-Le Coz, M., Chmeleff, J., Delpoux, S., Djouraev, I., Granier, G., Lacan, F., Piro, J.-L., Rousseau, T., Cloquet, C., Marquet, A., Menniti, C., Pradoux, C., Freydier, R., Vieira da Silva-Filho, E., Suchorski, K., 2019. A new interlaboratory characterisation of silicon, rare earth elements and twenty-two other trace element concentrations in the natural river water certified reference material SLRS-6 (NRC-CNRC). *Geostand. Geoanal. Res.* 43, 475–496. <https://doi.org/10.1111/ggr.12268>.
- Zheng, B., Ciais, P., Chevallier, F., Yang, H., Canadell, J.G., Chen, Y., van der Velde, I.R., Aben, I., Chuvieco, E., Davis, S.J., Deeter, M., Hong, C., Kong, Y., Li, H., Li, H., Lin, X., He, K., Zhang, Q., 2023. Record-high CO<sub>2</sub> emissions from boreal fires in 2021. *Science* 379 (6635), 912–917. <https://doi.org/10.1126/science.ade0805>.